Baharak Sajjadi*, Tetiana Zubatiuk, Danuta Leszczynska, Jerzy Leszczynski and Wei Yin Chen

Chemical activation of biochar for energy and environmental applications: a comprehensive review

https://doi.org/10.1515/revce-2018-0003
Received January 17, 2018; accepted May 28, 2018

Abstract: Biochar (BC) generated from thermal and hydrothermal cracking of biomass is a carbon-rich product with the microporous structure. The graphene-like structure of BC contains different chemical functional groups (e.g. phenolic, carboxylic, carbonylic, etc.), making it a very attractive tool for wastewater treatment, CO_2 capture, toxic gas adsorption, soil amendment, supercapacitors, catalytic applications, etc. However, the carbonaceous and mineral structure of BC has a potential to accept more favorable functional groups and discard undesirable groups through different chemical processes. The current review aims at providing a comprehensive overview on different chemical modification mechanisms and exploring their effects on BC physicochemical properties, functionalities, and applications. To reach these objectives, the processes of oxidation (using either acidic or alkaline oxidizing agents), amination, sulfonation, metal oxide impregnation, and magnetization are investigated and compared. The nature of precursor materials, modification preparatory/conditions, and post-modification processes as the key factors which influence the final product properties are considered in detail; however, the focus is dedicated to the most common methods and those with technological importance.

Keywords: amination; biochar; chemical activation; impregnation; magnetization; oxidation; sulfonation.

***Corresponding author: Baharak Sajjadi,** Department of Chemical Engineering, University of Mississippi, University, MS 38677, USA, e-mail: bsajjadi@olemiss.edu
Tetiana Zubatiuk, Danuta Leszczynska and Jerzy Leszczynski: Interdisciplinary Center for Nanotoxicity, Jackson State University, 1400 J. R. Lynch Street, Jackson, MS 39217, USA
Wei Yin Chen: Department of Chemical Engineering, University of Mississippi, University, MS 38677, USA

1 Introduction

The ordered structures of cubic diamond, hexagonal graphite, and the recently discovered hollow spherical form of carbon named as "fullerene", are the most known forms of carbon. However, most carbonaceous materials have less ordered structures, categorizing as graphitic and non-graphitic carbons. The latter is further classified into graphitizable (e.g. cokes derived from bituminous coals and crude oil) and non-graphitizable carbons, depending on the fluidity during pyrolysis. Biochars (BCs) are non-graphitizable carbon materials with highly developed internal porosity and surface area (Dalai and Azargohar 2007). These compounds are typically produced from the thermal or hydrothermal decomposition of oxygen-rich organic precursors, such as lignocellulosic biomass.

Lignocellulosic biomass consists of three major biopolymeric structures, known as cellulose, lignin, and hemicellulose, either of which has a unique and complex structure, as shown in Figure 1. Cellulose is a linear chain homopolymer constructed from glucose units [(1→4)-β-D-glucopyranosyl] with a varying degree of polymerization up to ~10,000. Hydroxyl groups on glucose units form intra- and intermolecular hydrogen bonds which result in the formation of a supramolecular structure with crystalline and amorphous domains.

Lignin is an irregular polyphenolic biopolymer consisting phenylpropanoid monomers with different degrees of methoxylation which are biosynthesized into a highly heterogeneous aromatic macromolecule. Hemicellulose is a branched polymer consisting of various sugar units of linked heteroglycans of pentoses and hexoses (mainly xylose and mannose; Figure 1) (Pu et al. 2013). The microfibrils in the cel1 walls include aligned cellulosic chains which are held together by hydrogen bonds between the hydroxyl groups of repeating glucose units. Groups of microfibrils make an array which is surrounded by a wall. Microfibrils are connected with each other by amorphous cellulose (~10–20% of the total cellulose) and hemicellulose and the arrays are intimately associated with each other by lignin and polysaccharides (a hemicellulose; Figure 1). The microfibrils in an array have a few nm space

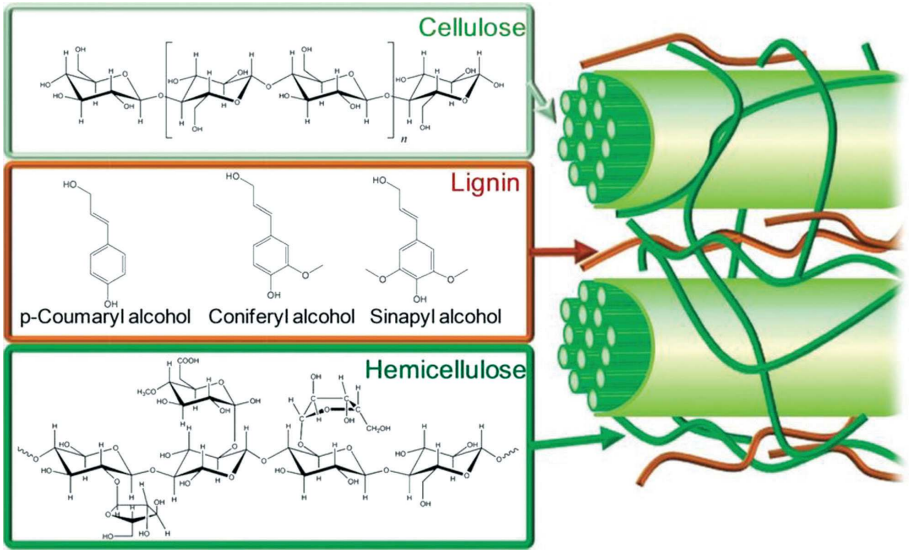

Figure 1: Lignocellulosic biomass structure (Copyright License No. 4332140852617, Chemical Society Reviews).

with each other which is in the same size of micro- and mesopore diameters (2–50 nm). A typical balance between the biopolymers content of biomass materials on a dry basis is: 40–60% cellulose, 20–40% hemicellulose, and 10–25% lignin (Yang et al. 2006).

While heated in the absence or under oxygen-limited conditions which is known as pyrolysis process, cellulose, hemicellulose, and lignin are broken down into smaller monomers through a series of complex reactions. Hemicellulose is the first to decompose (from ~200°C to 300°C) followed by decomposition of cellulose (beginning from ~300°C). If volatile compounds are simultaneously removed from the reaction medium, cellulose is mainly degraded to condensable organic vapors once 400°C is attained. The absence of ventilation and higher pressure assist the reactions of gases and formation of char at the expense of consuming condensable organic vapors. Lignin decomposes very slowly at a minor level in a wide range of temperature (160°C–900°C), yielding a solid residue (known as char) up to almost 40% of the original sample weight (Yang et al. 2006). These stable carbonaceous solids can be used in a wide range of applications. The most common applications of biomass-derived chars include soil amendments, adsorbents, metallurgical reductants, pigments, and fuels and have recently found potential uses in super-capacitors, lithium-ion batteries, composites, and structural materials. They also found a rapidly increasing application as a means of capturing carbon dioxide to prevent climate change and global warming. However, limited porosity, surface area, and polar oxygenated surface groups negatively affect the applications of BCs. Surface functionality provides favorable active sites for catalysis or pollutant adsorption processes while porosity and surface area facilitate mass transfer fluxes and are the effective factors for energy storage. The flexibility of BC materials is that porosity and surface area can be easily improved through physical modifications and functional groups can be easily tuned through chemical activations, and this offers a promising platform for synthesizing BCs with various desired properties. It should be noted that both processes have synergistic interactions too. Therefore, physical and chemical modification processes are commonly applied to enhance the performance of BC materials. Compared to physical treatment, chemical activation yields a higher activity, can be implemented at a lower temperature, and produces less amount of burn-off char. However, greater activity of BC and higher efficiency of the activation process is obtained at the expense of high cost of chemicals, difficult recovery of chemicals, and corrosion of the apparatus.

1.1 Acid/base sites on BC surface

The acidity or the basicity of BC surface has fundamental impacts on the adsorption of pollutants through acid-base reactions. As mentioned in our previous review on physical activation of BC (Sajjadi et al. 2018), the acidity/basicity of BC is governed by the randomly oriented polyaromatic clusters, heteroatomic surface functional groups, and mineral matters. The four to six layers of graphene-like crystalline clusters form the backbone of the BC produced at temperatures above 400°C (Kleber et al.

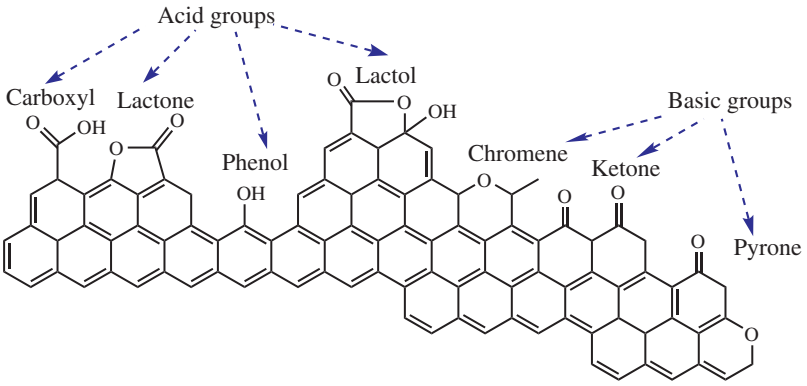

Figure 2: Proposed acidic and basic oxygen functionalities on carbon surfaces (Montes-Morán et al. 2004); Copyright License No. 4332160623409, Elsevier.

2015), which is similar to coal-derived char and petroleum coke. The delocalized electrons of the polyaromatic rings are considered Lewis bases. Most of the oxygen, nitrogen, sulfur, and hydrogen functional groups appear on the edge carbon of these clusters, though intercalated oxygen has also been reported.

The oxygen and nitrogen functional groups have been considered as the most influential factors governing carbon's surface acidity/basicity (Leony Leon and Radovic 1194, Boehm 1966, 2002, Radovic 1997, Radovic et al. 2001, Montes-Morán et al. 2004). Boehm (1966) classified the functional group into acid, base, and neutral type. As per their classification, oxygen-containing groups are mainly acidic (Figure 2) (Chiang et al. 2002).

Carboxylic acids, lactones, phenols, and lactol groups are the most known acidic groups which have been extensively characterized. However, not all oxygen-containing groups demonstrate acidic characteristics. As an instance, pyrones are the major oxygen functional groups governing the overall basicity (Montes-Morán et al. 2004). Exposure of heat-treated carbons to air leads to the formation of pyrones. Ab initio calculations have shown that the monocyclic ɣ-pyrone has low basicity ($pK_a \sim -1$). Nevertheless, the basic character of bicyclic pyrones is substantially higher than that of other surface oxide alternatives. Polycyclic pyrone-like model compounds cover a wide range of base strength (about 12 pK_a units). They react as basic centers through acid-base reactions according to the Brönsted definition. The main reason that explains the basicity of pyrone-like structures is the stabilization of the protonated form via the electronic π-conjugation throughout the sp^2 skeleton. Correlations of the thermal desorption products and desorption temperature during temperature-programmed desorption (TPD) have been reported by several groups, see Figure 3 (e.g. Figueiredo et al. 1999, Shafeeyan et al. 2010).

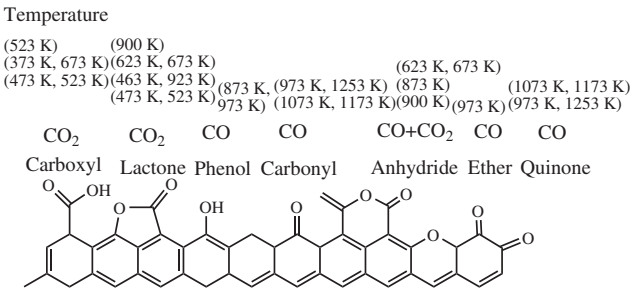

Figure 3: Surface oxygen containing groups on carbon and their decomposition by TPD (Figueiredo et al. 1999); Copyright License No. 4332151326404, Elsevier.

In general, acidic oxygen functional groups, such as carboxyl, lactones, and phenols sequentially decompose to CO_2 and CO when temperatures increase from 100°C to 700°C. Basic oxygen functional groups decompose above 600°C. Thus, most of the acidic oxygen functional groups could be removed from BC at high temperature and they are more susceptible to adsorption of acidic compounds.

Nitrogen-containing functional groups (e.g. amino group) mainly demonstrate basic characteristics. However, raw BCs produced from pyrolysis above 400°C are not likely to possess amino groups. Nitrogen atoms in raw BC are in the aromatic structure, i.e. the pyridine type. Montes-Morán et al. (2004) concluded that the nitrogen in the fused ring structure possesses basicity similar to bicyclic pyrenes. Aside from functional groups, basal planes in carbonaceous structure of BC demonstrated strong basic properties which is mainly due to hydrogen bonds between cations, H_3O^+, and π electrons on the basal planes (designated as -Cπ-H_3O^+ below), while counter-ions would be held at separated distances to satisfy electro-neutrality (Montes-Morán et al. 1998). The basic strength of the basal planes, however, seems to be much lower than that

of the pyrone-like groups (Montes-Morán et al. 2004). This is consistent with the reported pH of ultra-pure graphite in the range of 6.2–6.8. The delocalized π electrons on the basal planes are particularly important in adsorption of metal ions. As an instance, significant adsorption of Cd(II) (Sánchez-Polo and Rivera-Utrilla 2002) and Pb(II) (Machida et al. 2006) on an oxygenated surface including carboxylic acid and lactonic groups implies that electrostatic-type interactions predominate in the adsorption process. However, adsorption observed at solution pH values below the pH at the potential of zero point charge (pH_{pzc}) of the carbon indicates that other forces also participate in this process. The ionic exchange between -Cπ-H_3O^+ interaction protons and Cd(II), Cr(III), or Pb(II) ions would account for this observation.

Inorganic minerals in coal, biomass, and their chars include the salts of Na, Mg, Mn, K, and Ca (Xu et al. 2017). Mineral compounds are the basic sites which can also play important roles in adsorption of heavy metal cations in wastewater by Lewis acids/bases reactions. In other words, the adsorption sites for heavy metals are not only considered to be acidic surface functional groups on the external and internal surfaces but the basic mineral ash is also responsible for adsorption (Inoue et al. 1985, Machida et al. 2005).

1.2 BC surface charge

In chemisorption of contaminants in wastewater, surface functional groups, minerals in both BC and solution as well as solution pH have profound influences on the adsorption capacity. These factors govern the surface charge on BC and, in turn, redox potential and chemisorption of the BC surface. Consequently, the measurement of surface charge of carbonaceous sorbents by electrophoresis has emerged as a common practice in the effort to improve the adsorption capacity (see e.g. Hiemenz and Rajagopalan 1997). Dipole-induced polarity and dissociated surface groups are the two major origins of surface charges. Dipoles, organic and metallic, on an uncharged surface induce adsorption of ions such as H^+, OH^-, and metallic ions in a solution, producing a net charge on the surface. Surface charges can also be a result of dissociation of surface groups, such as carboxylic and phenolic groups. Thus, the pH and ions present in the solution can modify the organic and metallic surface groups and the adsorption of contaminants through these two mechanisms of surface charge formation. Moreover, pH can be used to adjust the surface ionic strength and rate of above mechanisms (Sumaraj and Padhye 2017).

ζ potential and pH at the pH_{pzc} characterize the electrophoretic mobility of particles in dispersion or molecules in solution. ζ potential is a measure of the electrostatic or charge repulsion/attraction potential energy between the adsorbent and the solution matrix. pH_{pzc} represents the pH where ζ potential equals zero suggesting no net electrostatic charges on the adsorbent; i.e. when the solution pH is higher than the pH_{pzc}, the surface exhibits negative charge (negative ζ potential) and higher adsorption of cation contaminants in the solution. Fundamental aspects of the interactions among surface functional groups, metal composition in the carbon, pH, and adsorbate was thoroughly reviewed by Leony Leon and Radovic (1194) and Radovic et al. (2001).

1.3 Classification of chemical activation

Chemical activation, in which char is doped with a chemical agent, is the most common method to modify surface functional groups, though its mechanism is not well understood. (I) In this process, the precursor (biomass) is impregnated with the chemical agent and then the mixture is thermally treated. During this process, the chemical agent dehydrates the sample, inhibits the tar formation and volatiles compounds evolution, and therefore increases the yield of the carbonization process. The distribution of chemical agents in the precursor prior to carbonization plays a key role in porosity development and functionality of the final products (El-Hendawy 2009). (II) Chemical activation can be typically conducted by soaking or suspending of a pyrolyzed BC in a chemical agent solution [at a ratio of up to 1:10 (BC: acids, base, salt)] at room temperature up to 120°C for a specific duration. A secondary thermal treatment may be used to obtain the desired modified BCs (Ahmed et al. 2016). Thermal treatment of functional group-rich char at high temperatures, carbonizes the organic matter completely, resulting in the formation of new nanopores, and the subsequent improvement in surface area (Nair and Vinu 2016). In both processes, BC is washed with acid or base and deionized water until the acidic/alkaline pH is neutralized; otherwise, the functionality and compatibility of BCs would be compromised. Washing also removes the chemicals left in the carbonized sample and generates new pores. The use of various reagents develops different surface functional groups. Hence, BC's chemical activation can be classified based on either the chemical agents or the functionalities obtained. In this review, the latter classification has been used since it comprises the benefit of the process and application of the produced BC (Table 1). Therefore, oxidation, amination, sulfonation, and impregnation

Table 1: A summary of activation methods and the applications.

Activation agent	Application	Comment
Modification/ activation with H_3PO_4	– Soil amendment – Wastewater treatment – Pesticides removal – Electrochemical energy storage	– The H_3PO_{4-} modified BC can increase concentrations of soil organic matter – H_3PO_{4-} modification increases the adsorption of positively charged ions such as methylene blue, heavy metals while negatively affects the negatively charged compounds in water (e.g. phenol) – High electron-donating ability of phosphorus dopant enhances the transport capability and charge storage of BC
Modification/ activation with HNO_3	– Wastewater treatment – Pesticides removal – Electrochemical energy storage – Electrochemical sensitivity	– HNO_{3-} modification increases the adsorption of positively charged ions such as methylene blue, heavy metals while negatively affects the negatively charged compounds in water (e.g. phenol) – The level of improvement in electrochemical energy storage is not as significant as by phosphoric acid treatment
Modification/ activation with HCl	– Wastewater treatment	– HCL treatment can increase the adsorption of basic contaminants such as methylene blue, hydrous metal oxides; heavy metals – HCL treatment can also increase the adsorption rate of N-containing compounds (e.g. nitrate, NO_3^-, and nitrite, NO_2^-) through anion exchange
Modification/ activation with H_2O_2	– Wastewater treatment – Soil amendment	– Oxidation of biochar surface with H_2O_2 can increase the adsorption of heavy metals – Free radicals generated through catalytic H_2O_2 conversion by biochar have fundamental importance to the oxidation of organic pollutants, remediation of contaminated soil, weathering of spilled crude oil, and toxicity of airborne pyrogenic particulate matters
Modification/ activation with $ZnCl_2$	– Wastewater treatment – Electrochemical energy storage	– $ZnCl_2$ treatment slightly improves the adsorptions of phenol and methylene blue – $ZnCl_2$ activation produces carbons with superior specific capacitances
Modification/ activation with KOH	– Soil amendment – Wastewater treatment – Electrochemical energy storage	– KOH-modified BC increases concentrations of soil organic matter – KOH-modified BC are efficient agents for removal of toxic metals, however KOH activation may reduce the level of exchangeable cations in biochar – Alkali modification with KOH significantly improves the adsorption of pesticides and phenols by reinforcing the π-π
Modification/ activation with NaOH	– Wastewater treatment – Electrochemical energy storage – Catalytic applications in the direct methanol fuel cell and methane storage	– High dosage of NaOH turns the micropores into mesopores, hence high dosage of NaOH increases the adsorption of larger molecular adsorbates while reduces the adsorption of small molecules – There are a fewer number of studies on applications of NaOH-modified biochar compared with KOH-modification
Sulfonation by H_2SO_4	– Catalytic applications – Heat-resisting applications – Oil absorbent	– H_2SO_4-treated biochars have a great potential to be used as an alternative route for homogenous H_2SO_4 catalysts
Amination by ammonia or amino-containing reagents	– Wastewater treatment – CO_2 capture	– Amine groups efficiently interact with CO_2 and increase the CO_2 capture capacity of biochar – Amine groups efficiently interact with metal ions and increase the adsorption of heavy metals on biochar
Impregnation With magnesium oxide	– Wastewater treatment – CO_2 capture	– MgO increases the removal of anionic nutrients, e.g. phosphate and nitrate – MgO is an effective adsorbent for the removal of heavy metals if the agglomeration of nano-sized MgO on carrier surfaces is eliminated – MgO-loaded biochar presented a reasonable performance in the CO_2 capture

Table 1 (continued)

Activation agent	Application	Comment
Impregnation with manganese oxide	– Wastewater treatment – Catalytic applications in degradation of gaseous pollutants – Electrochemical energy storage	– Both mineral structures of MnO (birnessite and manganosite) increase the adsorption of heavy metals on biochar – Specific capacitance of MnO_2-based supercapacitor depends on the particle size to a high extent – MnO_2 suffers from poor cyclic instability and electrical conductivity
Impregnation with calcium oxide	– Catalytic applications in transesterification – CO_2 capture – Gasification	– CaO-based catalysts suffer from leaching of CaO during the reaction – Calcium elements enhances the carbon retention and stability of biochar – Calcium elements increase the yield of gasification by $Ca(OH)_2$ mitigates the catalyst deactivation
Impregnation with Cu ions	– Wastewater treatment – Catalytic applications in catalytic wet air oxidation	– Few studies are available in wastewater treatment – CuO-modified biochar is stable and leaching of active sites is lower than commercial Cu-containing catalyst, improvement is still necessary
Impregnation with nickel oxide	– Electrochemical energy storage	– Thermal treatment of Ni-loaded biochar is necessary to convert Ni into NiO and NiOOH and improves the supercapacity of biochar
Impregnation with zinc oxide	– Wastewater treatment	– Zinc oxide can increase the adsorption of heavy metals by increasing the hydroxyl and carboxyl groups of biochar – Zinc oxide fastens and enhances the adsorption of dyes
Magnetization	– Wastewater treatment – Electrochemical energy storage	– Magnetic biochar provides effective adsorptivity and fast separation from water and are easily regenerated – Magnetic biochars can enhance the removal of metal ions and various aromatic pollutants

with nanomaterials as the main chemical modifications are reviewed here. Surface oxidation by using activating agents is the process normally used for creating oxygen-containing functional groups (OFG) on the surface of BC. Carboxyl, phenolic hydroxyl, lactones, and peroxides are the most common oxygen functional groups formed on BC after oxidation. Among these groups, hydroxyl and carboxyl groups remarkably improve the adsorption capacity when BC is utilized for heavy-metal removal. Oxidation can be accomplished by using either a gas such as steam, CO_2, ozone, air, or NO, during pyrolysis or treatment with an acidic/basic solution. The former is considered as the physical modification which was discussed in our previous work and the latter is the focus of the current review.

Basic amino moiety is a powerful complex functional group that efficiently adjoins to and removes CO_2 and pollutants (i.e. heavy metals). High-temperature treatment of BC in the presence of ammonia (NH_3) is the most commonly used method for the surface amination of BC. Chemical modification of BC surface with some amino-containing reagents can also be alternatively employed. Compared with these two methods, direct pyrolysis or hydrothermal cracking of nitrogen-rich biomass without the use of NH_3 or expensive chemical reagents is more sustainable. Notably, plasma treatment of BC in N_2 or NH_3 atmosphere is raising attention in the most recent works. Sulfonic ($-SO_3H$) groups are considered as the main functional group in solid acidic materials. Sulfonated-BC or activated carbon (AC) with a high density of sulfonic acid groups ($-SO_3H$) can be used as a noble alternative to H_2SO_4 in reactions like hydrolysis, esterification, and nitration. Nanomaterial impregnation is emerging as a new technology for improving the performance of carbonaceous compounds and increasing the selective sorption of target contaminant. The recent studies suggest that BC serves as a good platform for doping and immobilizing of nanomaterials such as aluminum, magnesium, manganese, iron oxide nanoparticle (NP), double-layered hydroxides, clay minerals, nano-zerovalent iron, and carbon nanotubes.

2 Oxidation

2.1 Acidic modification

Acidic additives catalyze the dehydration and elimination reactions occurring upon cellulose pyrolysis, suppress tar formation, and lower the pyrolysis temperature. Therefore, chemical changes and structural alterations in biomass including removal of oxygen, sulfur, and

hydrogen, increase in aromaticity, and loss of aliphatic character are promoted at lower temperatures. Research on the acidic treatment of BC has mainly been focused on using phosphoric acid, sulfuric acid, hydrochloric acid, and hydrogen peroxide.

2.1.1 Activation by phosphoric acid (H_3PO_4)

Phosphoric acid, as an efficient chemical activator, has been frequently applied to improve the property of carbon-based materials before or after the carbonization. Compared with the other acidic activating agents, H_3PO_4 has lower corrosivity and the products obtained contain less harmful residues, thus environmental benign.

2.1.1.1 At low temperatures

The reaction of phosphoric acid with biomass probably begins by the attack of acid to hemicellulose and lignin as soon as the components are mixed, even at low temperatures (50°C). Firstly, this happens because of the easier access to these amorphous biopolymers than to the crystalline cellulose. Secondly, it is feasible because of the resistant nature of cellulose to acid hydrolysis compared to other polysaccharides (Porter and Rollins 1972, Pandey and Nair 1974). The primary effects of acid attack include the hydrolysis of glycosidic linkages in hemicellulose and cellulose and cleavage of aryl ether bonds in lignin. Bond cleavage reactions accompanied by dehydration, degradation, and condensation results in the release of CO, CO_2, and CH_4, reduction in the molecular weights of hemicellulose and lignin, and formation of ketones in lignin. Dehydration reactions and H_3PO_4-promoted cleavage of ether linkages in cellulose and lignin are accounted for the appearance of carbonyl groups. The substantial release of CH_4 suggests that the cleavage of aliphatic side chains is relatively facile and is consistent with the loss of aliphatic character and increase in aromaticity. All these processes which contribute to the accelerated weight loss and volumetric contraction are observed for the water-insoluble char up to about 150–200°C. In such condition, phosphorus compounds form ester linkages with -OH groups on cellulose, crosslink the polymer chains, and introduce P atoms into the carbon matrix mainly as reduced states (Figure 4).

2.1.1.2 At intermediate temperatures

With increasing temperature (Figure 5), the rate of weight loss remarkably increases, and the structure begins to dilate which is correspondent to the development of porosity. However, crosslinking reactions initiated at lower temperatures gradually dominate over depolymerization and bond cleavage reactions. Therefore, treatment with phosphoric acid yields a higher carbon at temperatures above 300°C (Lim et al. 2010) due to crosslinking and retention of low molecular weight species in the solid phase.

Phosphoric acid also stabilizes the cellulose structure by inhibiting the formation of levoglucosan. Its

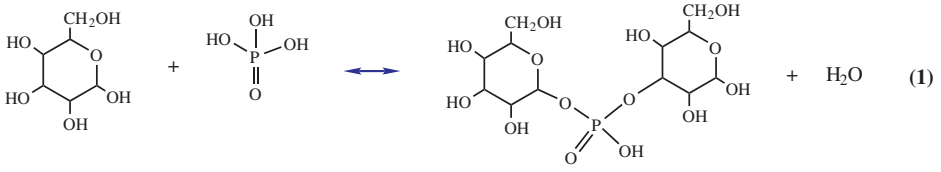

Figure 4: Formation of phosphate esters on cellulose side chains and crosslinking at low temperatures; Copyright License No. 4332180921365, Elsevier.

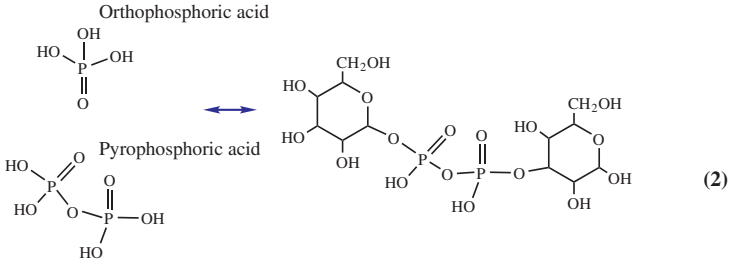

Figure 5: Esters can be derivatives of ortho-, pyro, and meta-phosphoric acids at intermediate temperatures; Copyright License No. 4332180921365, Elsevier.

decomposition to volatile products offers a route to substantial degradation of cellulose. The char structure produced between 280°C and 350°C consists of relatively small polyaromatic units, connected mainly by phosphate and polyphosphate bridges (swollen structure) that can include polyethylene linkages $(CH_2)_n$. Persistence of organic phosphor-carbonaceous inhibits the development of condensed polyaromatic structures at temperatures below 400°C (Pandey and Nair 1974). But the size of the polyaromatic units and aromaticity extensively grows at higher temperature due to the cleavage of crosslinks (scission of P-O-C bonds) which enable cyclization and condensation reactions. Thus, phosphoric acid plays two roles: (I) as an acid catalyst that promotes bond cleavage reactions and the formation of crosslinks via cyclization and condensation; (II) serves to connect and crosslink biopolymer fragments by being combined with organic species and converting to phosphate linkages. These groups are gradually hydrolyzed and/or oxidized by humidity and oxygen, leading to oxidized P-containing functional groups (such as C-O-PO_3 or $(CO)_2PO_2$) (Hasegawa et al. 2015). Generally, the structural dilation, which started from 150°C, up to the secondary cell walls' dilation at about 250°C, assists the micro- and mesopore development. It suggests that a portion of the final porosity arises from acid promoted reactions and the formation of phosphate esters with the amorphous biopolymers. Thickening of the secondary cell walls mainly contributes to developing the mesopores. Removal of the acid leaves the matrix in an expanded form with an accessible pore structure. The removal of carbon in the form of CO, CO_2, and CH_4 simultaneously assists the porosity development. Similar to that of the amorphous biopolymers, the expansion of crystalline cellulose ascribes to reaction with phosphoric acid that promotes chemical change including the stabilization of the cellulose chains, crosslinking through the formation of phosphate and polyphosphate esters, and crosslinking through the formation of etheric and other linkages. It should also be noted that due to the higher density and chemical structure of crystalline cellulose, its potential for the dilation is higher than that of amorphous polymers (Cameron and MacDowall 1983). Moreover, activation of crystalline cellulose produces a mixture of pore sizes while activation of the amorphous polymers produces mostly micropores. However, the porosity could be controlled by temperature and/or the ratio of acid to the precursor. More acid can incorporate into the structure at higher concentrations and the phosphate crosslinks become bulkier at a higher temperature; as a result, the mesopore volume increases (Cameron and MacDowall 1983, Jagtoyen and Derbyshire 1998).

2.1.1.3 Reaction at high temperature

The thickness of the secondary cell walls and the overall dimensions demonstrate that the structure begins to contract at temperatures above about 450°C (Figure 6). Different studies have shown that the reduction in the cell wall thickness between 450°C and 650°C is more significant than the overall contraction in the radial direction. Opposite of dilation which occurs by the formation of bulky phosphate linkages, contraction is consistent with their decomposition and since the phosphate bridges are more concentrated in the altered cellulose, breakdown exerts the greatest effect on this structure. Reduction in crosslink density contributes to rearranging the BC structure and increasing the aromatic cluster size, decreasing the porosity, and developing a more densely packed structure. Elimination of oxygen-containing groups and residual aliphatic is also observed in this range of temperatures.

In conclusion, H_3PO_4 activation not only introduces P-containing functional groups into the BC (Yang et al. 2011, Lin et al. 2012) but also increases the porosity by separating the microfibers through swelling phenomenon (Jagtoyen and Derbyshire 1993, Ahmed Hared et al. 2007, Patnukao and Pavasant 2008, Yang et al. 2011). However, the process is temperature dependent. The porosity of samples treated by phosphoric acid begins to develop at low temperature, increases sharply to a broad maximum, and decreases at a higher temperature while the range of temperature depends on the biomass source (Jagtoyen and Derbyshire 1993). If this process is

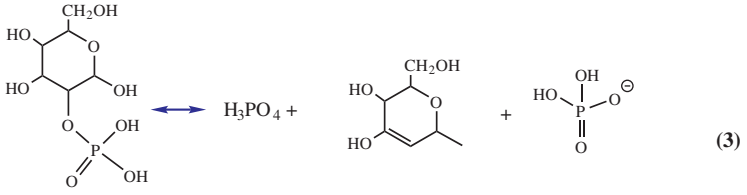

(3)

Figure 6: Elimination of H_3PO_4 at high temperatures; Copyright License No. 4332180921365, Elsevier.

followed by leaching in water, the acid is removed and is not retained in the expanded structure. Phosphate linkages which have a significant contribution to the total crosslink density have a strong affinity to water and are readily broken by hydrolysis in a matter of minutes at 100°C, allowing almost complete recovery of the acid. As a consequence, the structure becomes metastable. Volatile constituents that are no longer strongly bonded into the solid structure are subsequently removed by further heat treatment, widening the pore at the cost of reducing the carbon yield (Taha et al. 2014). Hence, a remarkable reduction in micropore volume and increase in mesopore volume are observed.

Chemical modification can also be applied after pyrolysis. In this process, phosphoric acid quickly diffuses to the outer part of the particles and dissociates the weakly bonded components (e.g. labile carbon and volatile matter). If the process proceeds with thermal treatment, the reaction of C with H_3PO_4 molecules follows as $4H_3PO_4 + 10C \rightarrow P_4 + 10CO + 6H_2O$, therefore etching of C with H_3PO_4 develops a high quantity of porosities (Sun et al. 2015). High impregnation ratio or activation temperature (if the process is followed by a thermal treatment) considerably expands the porous structure of the synthesized AC, lowering micropores while creating more meso- and macropores (Tsang et al. 2007). On the other side, a part of carbons is oxidized by phosphoric acid creating new functional groups on the surface and inside the pores. Increase in the number of -OH and particularly -COOH groups as well as the formation of new functional groups such as P=O, P=OOH and P-O-P have frequently been demonstrated (Figure 7). These new groups may result in a slight reduction in the surface area due to blockage of some microspores if no thermal treatment is applied (Almeida et al. 2017).

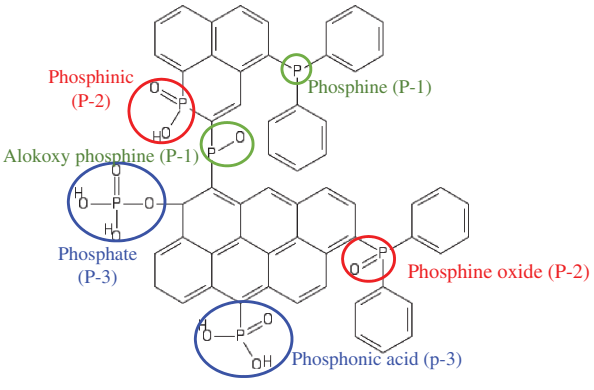

Figure 7: P-containing functional groups in the carbon matrix (Elmouwahidi et al. 2017), Copyright License No. 4332180146879, Elsevier.

2.1.1.4 Application

H_3PO_4-modified BC has particular application as a soil amendment (Zhao et al. 2016). The modified BC can increase concentrations of soil organic matter, especially water extractable organic carbon (WEOC) possibly by promoting hydrolysis reactions on BC surfaces (Lin et al. 2012). Modification in the presence of H_3PO_4 also improves the performance of BC in adsorbing inorganic contaminants from wastewater via surface adsorption, carboxyl functional group retention, and co-precipitation with phosphorus (Tsang et al. 2007). The strongly negative surface of the modified BC due to the presence of new oxygen/phosphorous-containing functional groups facilitates the adsorption of positively charged ions such as methylene blue, heavy metals [e.g. Cu(II) and Cd(II) (Peng et al. 2017)] while negatively affects the negatively charged compounds in water (e.g. phenol) (Liu et al. 2008). Phosphoric acid-treated BC can also easily remove pesticides, especially those with a high degree of hydrophobicity, from contaminated water through primary π-π dispersive interactions, the highly polar bonds (C-F, P=S, and PO) (Taha et al. 2014), and van der Waals forces. Moreover, there is a strong interaction through hydrogen bonding between the polar groups of polar pesticides with the acidic surface of the H_3PO_4-modified BC, which contains more number of hydroxyl groups.

H_3PO_4-modified BC products would also present alternative species with a strong ability in electrochemical energy storage. Phosphorus compounds have demonstrated strong pseudo-capacitance with favorable stability. Moreover, high electron-donating ability of phosphorus dopant remarkably enhances the transport capability and charge storage of carbonaceous materials. Experimental results showed that phosphorus-rich carbons could yield 3–20 times higher specific capacitances compared with pristine BC (Hulicova-Jurcakova et al. 2009). The P-doped carbon electrode presents a long-term cycling durability as well (Yi et al. 2017). It attributes to the significant role of phosphoric acid in increasing the surface area, porosity, and oxygen/phosphorous functionalities. However, there are very few studies on this topic.

2.1.2 Activation by nitric acid (HNO_3)

Concentrated nitric acid is one of the other common oxidizing solutions. HNO_3 treatment increases the quantity of structures containing N-O bonds (nitro groups and nitrate complexes). The reaction between aromatic carbon structures and HNO_3 and the generation of nitrate (NO_3^-) and nitrite (NO_2^-) ions have been proved in this process.

Formation of surface functional groups during the reaction between the HNO_3 solution and carbonaceous structure follows a complex temperature-dependent mechanism. It has been proved that the oxidizing agents in a nitric acid solution include HNO_3, $(OH)_2NO^+$, NO_2^+, NO_3^-, H_3O^+ which form during reduction.

2.1.2.1 At low temperatures

Oxidation and nitration are the two reactions occurring during activation with nitric acid. For the former, a series of oxygen addition and dehydration reactions leads to oxidation of aromatic rings with nitric acid. In this process, aromatic ring opens and forms two carboxyl groups, through the well-known classical reaction of coal nitric acid oxidation (R4) (Figure 8). Therefore, oxidation with nitric acid results in the increase of oxygen content and carboxyl group in the nitric acid oxidized coal and decrease of aromaticity (Shi et al. 2012). Increasing temperature up to 100°C plays a key role in the formation of more carboxyl structures and OH group (Figure 9).

Aside from oxidation of aromatic rings, aliphatic side chains on the AC surfaces are also susceptible to oxidation and formation of ester, aldehyde, or alcohol (Chen and Wu 2004). Oxidation of side chain increases the contents of oxygen and aliphatic carbon but reduces methyl carbon and side chain length (CH_3/CH_2).

In terms of nitration, the active point of nitration reaction is NO^{2+}, which is generated by the below reactions:

$$HNO_3 + HNO_3 \leftrightarrow H_2NO_3^+ + NO_3^-$$
$$H_2NO_3^+ \leftrightarrow NO_2^+ + H_2O$$

Nitration of aromatic rings is an electrophilic substitution reaction which increases the contents of N and O elements in the modified BC (Zawadzki 1980, Yakout 2015). In this reaction, NO^{2+} is first added to aromatic rings to form σ combination and then forms the nitro group by deprotonation reaction. The carbonaceous aromatic structures reacting with HNO_3 may also form an organic structure containing nitro-oxygen groups (Yakout 2015). It seems that of -O-NO_2 complex species can be formed on carbon presenting active sites (O-containing surface groups) with only one oxygen atom (e.g. phenolic groups or ketones and quinones) (Ghouma et al. 2017).

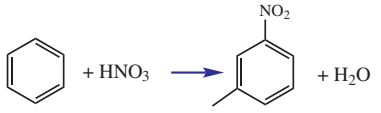

(6)

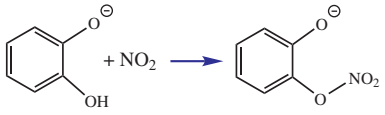

(7)

Organic nitrates and surface nitrate complexes are relatively unstable, though they do not decompose during the desorption at room temperature, partially decompose when desorbed at 200°C and completely disappear when

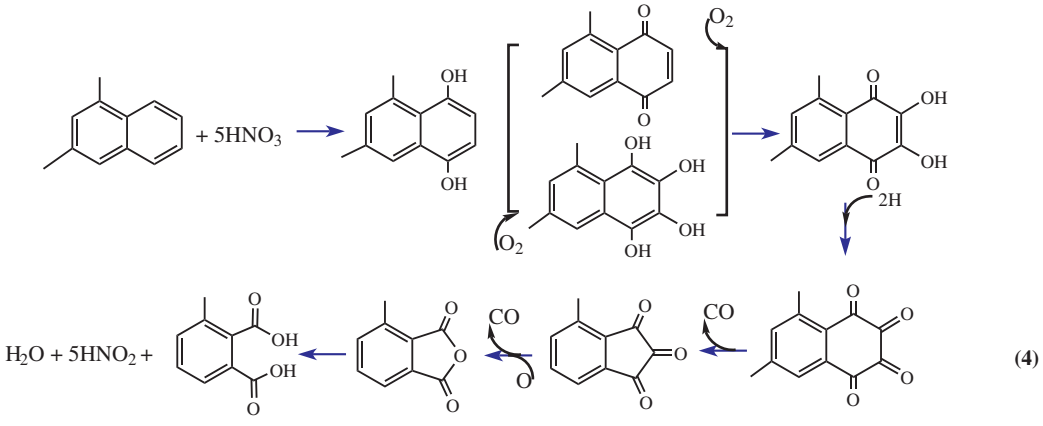

(4)

Figure 8: Classical reaction of nitric acid oxidation (Shi et al. 2012).

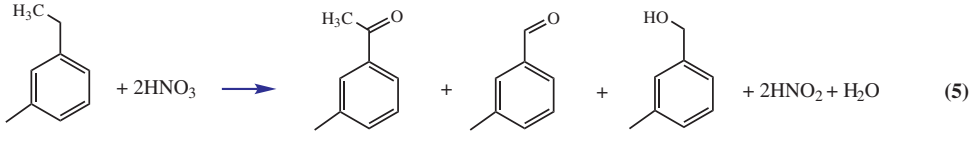

(5)

Figure 9: Oxidation of aromatic rings by nitric acid (Shi et al. 2012).

desorbed at 400°C. The thermal decomposition of surface structures containing nitrogen-oxygen bonds is accompanied by intramolecular rearrangements (of Iono-radical structures C.-.O probably) with the formation of carbonyl groups. Iono-radical structures are in fact an intermediate stage in the process of formation of C=O as shown below (Zawadzki 1980).

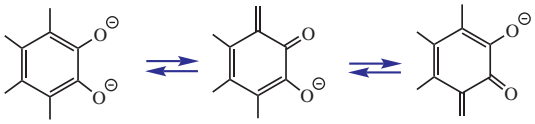

(8)

2.1.2.2 At high temperatures

Oxidation degree through HNO_3 treatment rises at higher temperatures (~800°C), resulting in thermal decomposition of aliphatic C-H structures and a high substitution degree of aromatic rings by oxygen groups (Zawadzki 1980, Yakout 2015). Hence, it can be noted that the strong oxidative nature of HNO_3 promotes the removal of carbon atoms, lowering the carbon yield (Foo and Hameed 2012a). Oxidation of BC becomes more severe with a higher concentration of nitric acid. Therefore, the carbon and hydrogen contents decrease, while the amount of oxygen and nitrogen increase. The decrease of carbon results from the destruction of the pore walls and the increase of nitrogen and oxygen results from the formation of aromatic compounds containing nitrogen and carbon-oxygen functional groups on the surface (Güzel et al. 2017).

HNO_3 as a simple inorganic acid with a small molecular weight does not cause a significant change in the specific surface area of carbons (Chen and Wu 2004). However, it dissolves the inorganic substances. BC contains either inorganic substances with low chemical reaction abilities as well as active components such as SiO_2, Al_2O_3, Fe_2O_3, K_2O, and Na_2O and some impurities such as CaO and MgO which are able to react with HNO_3 (Liu et al. 2012). As an instance, HNO_3 reacts with solid Fe_2O_3 and forms soluble $Fe(NO_3)_2$. With the solubilization of such components, other accompanying inorganic substances lose their adhesive force support and are separated from BC. Therefore, the pore sizes, pore volumes, and surface area slightly increase at an early oxidation stage. However, the crystallites are coagulated and carbon layers are broken up as the oxidation proceeded and hence changes of porosity and surface area became negligible (Kamegawa et al. 1998). Total acidity of the surface which resulted from the increase in surface acidic functional groups keeps increasing with nitric acid concentration or oxidation duration (Jaramillo et al. 2009, Güzel et al. 2017). Hence, micropores are narrowed or blocked by oxygen groups formed on the entrance and walls of pores. Interestingly, even the mesopore volumes decreased during strong oxidation and the conversion of micro- and mesopores to macropores was reported (Gokce and Aktas 2014).

2.1.2.3 Application

The improvements in the specific surface area, pore size distribution, porosity structure, electrical conductivity, and surface functional groups after HNO_3 treatment affect the electrochemical performance, pollutant removal, and electrochemical sensitivity of carbon materials. With the particular focus on electrochemical performance, surface oxidation with HNO_3 treatment improves the capacity of the carbonaceous structure in supercapacitor. Besides the addition of surface oxygen groups and increase of pore size and volume, HNO_3 oxidation might also introduce nitrogen groups into the BC structure, which have been proved to increase the capacitance of electrodes by inducing Faradaic reactions (Jin et al. 2013). However, the level of improvement is not as significant as by phosphoric acid treatment.

Surface oxidation after HNO_3 treatment enhances the sorption capacity of heavy metals by BCs too. As an example, cottonseed hull-, wheat straw-, and cow manure-derived BCs were found to be rich in carboxyl groups after HNO_3 treatment and demonstrated remarkably greater Pb, Cu, Zn (Uchimiya et al. 2012), and U(VI) (Jin et al. 2018) retention ability than the untreated BCs. Removal of other positively charged ions (e.g. methylene blue) has also been improved after nitric acid treatment (Güzel et al. 2017). The interaction between BC and pesticides has frequently been reported in the literature. As already mentioned, π-π and hydrogen bonds make the basis of sorption mechanism of pesticides on BC. Knowing this, de Oliveira et al. (2017) used an electrode modified with BC activated with nitric acid for quantitative determination of methyl parathion (MP pesticide) in drinking water. The new electrode with the limited detection rate of 0.1–70 μmol l^{-1} showed 65% higher sensitivity to MP compared with electrode constructed from non-activated BC, respectively.

2.1.3 Activation of BC by hydrochloric acid (HCl)

Hydrochloric acid with Ka of $1.3e^6$ is among the very strong mineral acids ($K_a(H_2SO_4) = 1e^3$, $K_a(HNO_3) = 2.4e^1$, $K_a(H_3PO_4) = 7.1e^{-3}$). In the preparation of activated BC, HCl solution has been adopted in the different stages of the activation for different purposes.

Generally, weaker acidic functional groups are deprotonated at a higher pH while stronger acidic functional groups are deprotonated at a lower pH. Therefore, HCl treatment increases the quantity of weak acidic oxygen functional groups and single-bonded oxygen functional groups such as phenols, ethers, and lactones (Chen and Wu 2004, Tong et al. 2016). A possible mechanism is the constitution of one basic site from two neighboring oxygen atoms, resulting in the formation of a pyrone-type structure. Positions of these two atoms in two different rings of a graphitic layer favor resonance stabilization of the positive charge (Chen and Wu 2004).

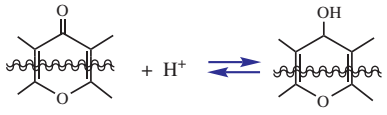

(9)

It further supports this theory that HCl does not generate new functional groups but converts carbonyl or carboxyl groups to phenol or lactone groups. Moreover, HCl treatment increases the oxygen content of carbonaceous structure which is possible through the chemisorption of water molecules by delocalized π electrons in the carbon basal plane. Indeed, pH reduction of carbon surface confirms this theory.

$$C_{\pi} + H_3O^{+} \leftrightarrow C_{\pi} - H_3O^{+} \tag{10}$$

where C_{π} denotes a carbon surface platelet having maximum itinerant π electrons.

Dilute HCl solution (almost 0.001 M HCl) is often used to remove the precipitated salts and impurities from the pores of carbonaceous sorbent (Zhang et al. 2007). On the other hand, HCl and HNO_3 are simple inorganic acids with small molecular weights. Such acids cannot be adsorbed by organic functional groups of carbonaceous structure and do not significantly change the specific surface area of carbons (Chen and Wu 2004). However, they can slightly increase the surface area and pore volumes by opening the blocked pores.

2.1.3.1 Application

During activation of carbons for adsorption, HCl removes salts from the pores, swells the organic and inorganic substrates, and induces positive charges to the sorbent surface. These features are beneficial to the adsorption of organic and inorganic contaminants from aqueous solutions, especially those basic contaminants such as methylene blue, nitrate, and hydrous metal oxides. HCl treatment or pH adjustment by HCl during adsorption enhances the adsorption of Cd(II), Cu(II), Cr(III), Cr(VI), Ni(II), Pb(II), Zn(II), As(III), and As(IV). These metal cations in water, as well as at the carbon surface, often appear in their hydrous forms. Thus, the adsorption process is often governed by the interactions among these hydrous metal oxides and hydrated carbon surface, which in turn, are influenced by pH of the solution. The review by Radovic et al. (2001) contains a thorough and systematic introduction to these fundamentals. Generally, BC treatment with low HCl concentration (up to almost 5 M) increases the trace metal adsorption. In terms of Cd(II), Cu(II), Ni(II), Pb(II), and Zn(II), the adsorption uptake of HCl BC increases with pH (Low et al. 2000, Nasernejad et al. 2005, Argun et al. 2007) while opposite trend is observed in terms of Cr(III) and Cr(VI) (Nasernejad et al. 2005, Argun et al. 2007). However, best adsorption of all heavy metals is observed in acidic range (pH < 7). Argun et al. (2007) suggested that Cu(II) and Ni(II) form chelates on the protonated carboxylic and phenolic groups of HCl-treated biomass:

$$R(OH)_2 + M^{+2} + H_2O \rightarrow ROM + 2H^{+} + H_2O \tag{11}$$

In the adsorption of Cr(VI), the following species: H_2CrO_4, $HCrO_4^{-}$, $Cr_2O_7^{-2}$, and CrO_4^{-2} are all present in the aqueous solution. Argun et al. (2007) stated that the major anion in the solution at pH 3 is likely to follow the reaction similar to that proposed by Park and Jang (2002) for the adsorption of Cr(VI) on BC treated by 35% HCl.

$$ROH + HCrO_4^{-} + H^{+} \rightarrow RHCrO_4 + H_2O \tag{12}$$

The adsorption is endothermic suggesting chemisorption nature of the process. However, the concentrated HCl (37% ~12.036 M) contains a certain amount of Cl_2. Hence, the changes imposed to the functional groups through the nucleophilic substitution, the Hell-Volhard-Zelinsky reaction, and the Markovnikov additions may negatively affect the reduction of metal adsorption capacity by following the reactions below:

$$R\text{-}OH + HCl \rightarrow RCl + H_2O \tag{13}$$

$$RCH_2COOH + Cl_2 \rightarrow RCHClCOOH + HCl \tag{14}$$

$$RCH = CH_2 + HCl \rightarrow RCHClCH_3 \tag{15}$$

$$RCH = CH_2 + Cl_2 \rightarrow RCHClCH_2Cl \tag{16}$$

Acid (herein, HCl) treatment produces higher proton charge on the carbon surface, leading to a higher electron ionization with anions in the aqueous solution, such as nitrate and nitrite. Protonated carbon surface serves as anion exchange sites in adsorption, a concept demonstrated by Orlando et al. (2002). In their work, they

revealed the high adsorption capacity of agricultural residue after creating anion exchange sites on the surface of natural cellulose after replacing the hydroxyl groups with protonated amine (i.e. ammonium ion). Increase in adsorption rate and capacity of N-containing compounds (e.g. nitrate, NO_3^-, and nitrite, NO_2^-) by HCl-treated BC has been a focal subject of several studies. Interactions of surface functional groups of BCs with inorganic nitrogen compounds have significant impacts on a number of inter-related reaction subsystems in plant/soil/water/BC systems (Afkhami et al. 2007). These subsystems include (I) the conversion of organic N to inorganic N (or mineralization), (II) immobilization of N on plants through microorganisms, (III) nitrification through reduced temperature variation and improved water retention due to the presence of BC, (IV) denitrification in the formation of N_2O due to the addition of BC, and (V) conversion of N_2 to NH_3 by nitrogen fixation bacteria, diazotrophs. The complex mechanisms of these reactions render the discussion of interactions of BC inorganic N a topic of several recent reviews (Nguyen et al. 2017, Sumaraj and Padhye 2017). HCl treatment of BC has also been used in adsorption of basic dyes, such as methylene blue (MB), which was found to be endothermic (Mahmoud et al. 2012). The adsorption capacity increases with pH (with the optimal adsorption in basic ranges, $pH > 7$), which can be explained by the MB's ability to capture multiple protons during the pH adjustment. Thus, in aqueous solutions, the three nitrogen and one sulfur atoms in MB cation represent all sites for proton association, which are acidic in nature. At higher pH, MB cations are less protonated and more susceptible to the acidic BC surface (Lewis and Bigeleisen 1943).

2.1.4 Activation by hydrogen peroxide (H_2O_2)

Hydrogen peroxide, H_2O_2 or HOOH, has a single bond between two oxygen atoms. It is an oxidizer, disinfectant, and decolorizer. It is unstable and decomposes during storage and in the presence of catalysts. Thermal decomposition of hydrogen peroxide yields O_2 and H_2O, which can be catalyzed by most transition metals, their oxides and enzyme catalase. Certain metal ions, such as Fe^{+2} and Ti^{+3}, catalyze the conversion of H_2O_2 to HO· and HOO· radicals. These strong oxidizing free radicals play the central role in oxidizing the pollutants in contaminated water. Catalytic conversion of H_2O_2 by ACs has been widely reported (Georgi and Kopinke 2005). Moreover, direct contact of H_2O_2 and carbonaceous materials creates surface oxides on the carbon-based sorbents, which enhances the pollutant-capture capacity. Thus, BC's surface plays two types of roles in BC/H_2O_2/pollutant/water systems: adsorption of pollutants through H_2O_2-induced surface oxides and catalytic H_2O_2 conversion to hydroxyl free radical (Santos et al. 2009), which are the focus of our discussion below. The relative importance of these two mechanisms is complex and still under active investigation. In practice, catalytic H_2O_2 conversion has the advantage to avoid the need to treat the spent sorbent that contains contaminants in the original aqueous phase.

2.1.4.1 H_2O_2-induced surface oxides

The ability of hydrogen peroxide (H_2O_2) for BC oxidization has not been systematically investigated and there are very few studies on this field, most of which suffer from lack of strong discussion. H_2O_2 in water dissociates forming O_2H^- and H^+ at low temperature. The pKa is 11.75, implying that the base form is more reactive. As per most studies, H_2O_2 oxidation increases the quantity of carboxylic, lactone, and hydroxyl group, among which the amount of hydroxyl group linearly increases with H_2O_2 concentrations (Zuo et al. 2016). H_2O_2 consistently decomposes the aromatic carbons comprising of two different products (i) aliphatic carboxylic acids and (ii) CO_2 and H_2O (Xue et al. 2012, Zuo et al. 2016, Cibati et al. 2017). Therefore, carboxylic significantly increases (up to 4 times) with H_2O_2 treatment. In the long oxidation duration with H_2O_2 of low concentration, after the initial increase of carboxylic and lactone groups, a slight reduction is observed indicating that the aliphatic carboxylic acid is the dominant decomposition product too (Zuo et al. 2016). The changes due to H_2O_2 treatment occur mostly on the surface, and therefore do not have a significant effect on a bulk property such as porosity.

If BC modification with H_2O_2 is followed by a thermal treatment, hydrogen peroxide adsorbed onto the surface and mesopores of the untreated BC decomposes into H_2O and O_2. Moreover, hydrogen peroxide directly reacts with the carbonaceous structure, resulting in the formation of gases such as CO, CO_2, and H_2 through the following reactions:

$$2H_2O_2 \rightarrow 2H_2O + O_2 \tag{17}$$

$$H_2O_2 + C \rightarrow H_2 + CO_2 \tag{18}$$

$$H_2O_2 + 2C \rightarrow H_2 + 2CO \tag{19}$$

Evolution and release of these gases significantly improve the porosity and surface area of the modified BC (Nair and Vinu 2016).

2.1.4.2 Catalytic H_2O_2 conversion to hydroxyl free radical

BC and hydrogen peroxide have a two-way interaction with each other. On one hand, H_2O_2 oxides BC, but on the other hand, H_2O_2 decomposes over carbon surface and forms free radical, which is an effective application of BC to degrade environmental contaminants. While the HO· free radical plays key roles in oxidizing and degradation of aqueous organic contaminants, its half-life is extremely short, approximately 10^{-9} s (Khachatryan et al. 2011). Consequently, the formation and reaction mechanisms of HO· free radicals and other reactive oxygen species (ROS) such as superoxide ion, $\cdot O_2^{-1}$, and hydroperoxyl free radical, $\cdot O_2H$, have been a focal topic of many studies. Though most studies have focused on the catalytic redox reactions that resemble the Fenton reactions ($Fe^{+2} + H_2O_2 \rightarrow F e^{+3} + HO\cdot + OH^{-1}$ and $Fe^{+3} + H_2O_2 \rightarrow Fe^{+2} + HOO\cdot + H^{+1}$) which generates hydroxyl free radical, hydroperoxyl free radical, while catalytic redox reactions can produce persistent free radicals (PFRs) as well. These resonance-stabilized PFRs include semiquinones, phenoxyls, and cyclopentadienyls. In the presence of metal oxides, such as CuO and Fe_2O_3, these PFRs are formed by thermal decomposition of catechols, hydroquinones, and phenols (Dellinger et al. 2007). These PFRs are stable, resist to oxidation, and have notably high concentrations of unpaired spins, which in turn, induce the sustained formation of ROS with very long half-lives, in the order of hours, days, or even infinitely long (Lomnicki et al. 2008). For instance, the PFR concentrations in pyrogenic carbonaceous particulate matters, $PM_{2.5}$, is about 10^{16}–10^{17} unpaired spins per gram of $PM_{2.5}$; they are stable for several months (Squadrito et al. 2001). Figure 10 illustrates the conversion of a substituted aromatic compound to a phenoxyl-type PFR on a metal surface (Lomnicki et al. 2008), which is sufficiently general for pyrogenic particulates including BC. PFR formation proceeds through a mechanism of (1) physisorption and (2) chemisorption by the elimination of HX, and

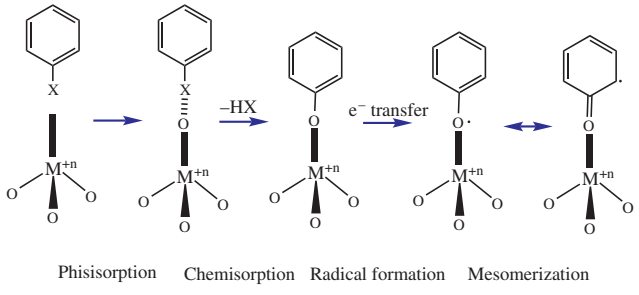

Figure 10: Mechanism of formation of a phenoxyl-type PFR from a substituted aromatic on a metal oxide surface (Balakrishna et al. 2009), copyright license: Balakrishna et al.; licensee BioMed Central Ltd. 2009 (Lomnicki et al. 2008).

electron transfer to form the surface-associated PFR and a reduced metal. The resulting radical may be primarily oxygen-centered or carbon-centered based on the properties of the PFR-metal complex.

When the mechanism discussed in Figure 10 is applied to BCs, a high concentration of PFRs (about 10^{16}–10^{18} unpaired spins per gram of BC) along with hydroxyl radicals can be quantified in BC/H_2O_2/H_2O systems (as per Figure 11) (Fang et al. 2014a,b). Moreover, there are linear relations among H_2O_2 concentration, hydroxyl radical concentration, and its degradation effect.

Aside from formation of PFRs, BC or AC catalyzes the conversion of H_2O_2 to HO· with the overall reaction that resembles the Fenton reaction discussed earlier:

$$AC + H_2O_2 \rightarrow AC^+ + HO\cdot + OH^{-1} \quad (20)$$

$$AC^+ + H_2O_2 \rightarrow AC + HOO\cdot + OH^{+1} \quad (21)$$

Positive correlations have been reported between the AC's free radical concentration and HO· concentration. Moreover, the decomposition rate of H_2O_2 is proportional to the concentration of hydroxyl group on the BC surface.

The proposed mechanism of HO· generation is that FRs in BC transfer electrons to O_2 to produce ROS, such as the superoxide radical anion and hydrogen peroxide, which disproportionate to H_2O_2. The subsequent back reaction of H_2O_2 with BC, possibly aided by transition metals in BC, generates HO·, which enhances the DEP degradation. A similar pathway was demonstrated for system supplemented with peroxydisulfate, which generates sulfate radicals as well (Fang et al. 2015a,b).

The role of adsorption of contaminants on BC or AC has also been a focus of different studies. Georgi and Kopinke (2005) investigated the degradation rate constants of methyl tert-butyl ether (MTBE), trichloroethene (TCE), and 2,4,5-trichlorophenol (TCP) in the AC/H_2O_2 system and those in the homogeneous. Their research revealed that the predominant pathway for the degradation in the AC/H_2O_2 system is the reaction of HO· with the organic contaminants in an aqueous phase. The adsorbed contaminant is nearly unreactive with the HO·. As a result, adsorption is detrimental to degradation by HO·. In contrast, Yang et al. (Yang et al. 2016a,b, 2017) recently challenged the "simplified" theory discussed above and claimed that HO· and liquid phase reactions are playing the major roles in the degradation of p-nitrophenol (PNP) in the BC/H_2O/PNP systems with and without H_2O_2. However, adding a radical scavenger, such as tert-butanol, did not completely inhibit PNP degradation suggesting that HO· is not solely responsible for the PNP degradation.

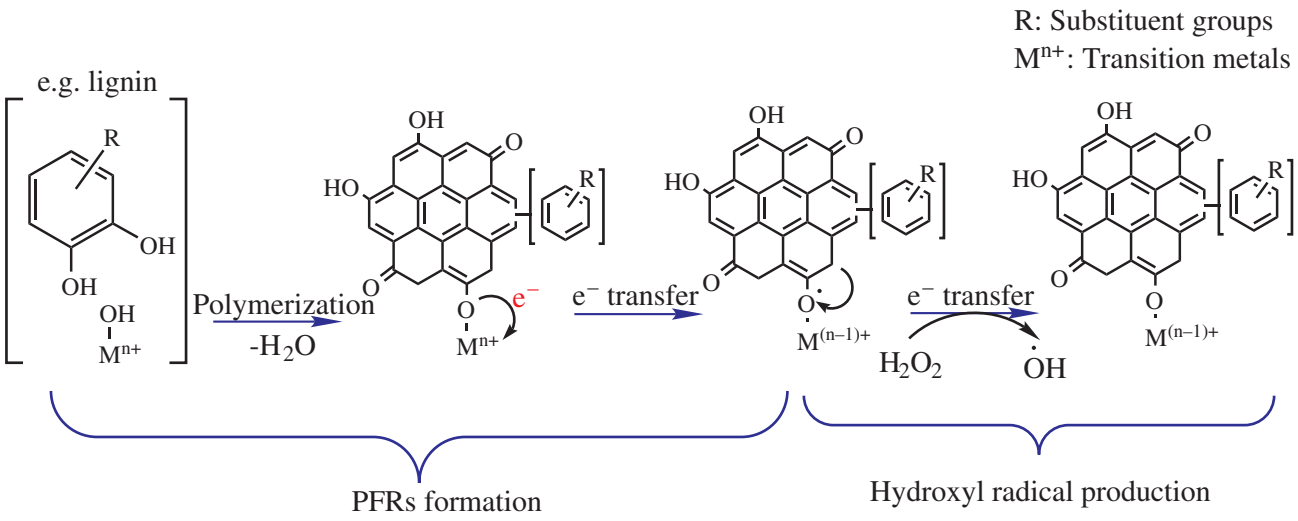

Figure 11: Proposed mechanisms of PFR formation and H_2O_2 activation by biochar (Fang et al. 2014a,b), with copyright license, American Chemical Society.

The decreased PNP degradation after tert-butanol addition was better correlated with reduced PNP sorption on BC, indicating that surface reaction of PNP with PFRs is likely an important contributor to the PNP degradation. Figure 12 presents their proposed mechanism. The mechanisms involving BC, its PFRs and ROS discussed above depend on the biomass' origin, thermal history and their physical and chemical interactions.

2.1.4.3 Application

Generally, significant increase in oxygen-containing functional groups using H_2O_2 treatment increases the cation exchange capacity of the modified BC, assisting the removal of heavy metals, e.g. Cu (II) (Zuo et al. 2016), Zn(II) (Cibati et al. 2017), Pb, Cd, and Ni(II) (Xue et al. 2012). The three oxygen-containing functional groups (carboxylic, hydroxyl, and lactone) are mainly responsible for metal removal by H_2O_2-modified BC, while the changes in specific surface area and surface structure do not play a significant role. Contrarily, high amount of oxygen weakens the overall dispersive forces of π-π interactions that are mainly responsible for the adsorption of dyes onto aromatic units of BC. As an example, Huff and Lee (2016) reported the lower methylene blue adsorption capacity with the higher H_2O_2 concentration treatments.

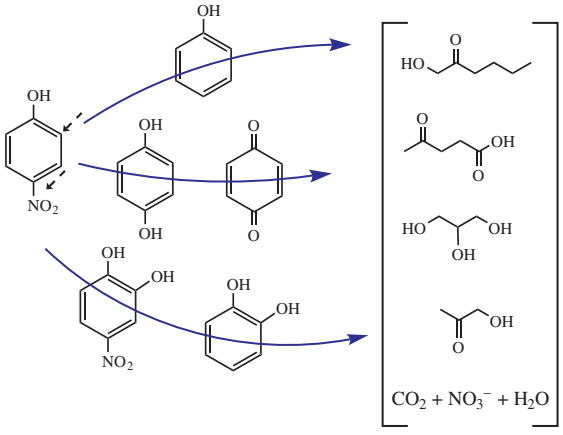

Figure 12: Schematic diagram of PNP degradation by PFRs through biochar sorption systems (Yang et al. 2016a,b), with copyright license, American Chemical Society.

On the other hand, generation of hydroxyl free radicals through catalytic conversion of H_2O_2 over carbon surface have fundamental importance to several distinct fields: the oxidation of organic pollutants in water treatment (Fang et al. 2014a,b, 2015a,b), remediation of contaminated soil, weathering of spilled crude oil, and toxicity of airborne pyrogenic particulate matters (PM) in biological systems (Lomnicki et al. 2008). As an example, polychlorinated biphenyls are an important group of persistent organic pollutants. Experimental results on activation of H_2O_2 by BC demonstrated 95% degradation of 10.6 μM 2-CB, while no obvious loss of 2-CB was observed in control experiments by H_2O_2 without BC. Investigating the mechanism of this degradation indicated that PFRs are the main contributor to the formation of ·OH (Liao et al. 2014) and subsequently, ·OH is the main contributor to 2-CB degradation (Fang et al. 2014a,b). The mechanisms of free radical generations in BC/H_2O_2/water systems, the oxidization of BC surface in this system, and their applications are still hot topics that need more systematic studies.

2.1.5 BC modification with $ZnCl_2$

$ZnCl_2$ as a Lewis acid is able to interact with non-bonding electrons of oxygen atoms, e.g. OH groups in the precursor (herein biomass), and hence the absence of such electrons reduces the activating ability of $ZnCl_2$. In other words, the $ZnCl_2$ impregnated on biomass remains in its crystallized form even after carbonization. During the impregnation step, degradation of biopolymers (cellulose, lignin, and hemicellulose) in biomass structure is promoted by high acidity of the $ZnCl_2$. This Lewis acid reacts with the OH functional groups in the biomass and forms Zn-O complexes, subsequently followed by the elimination of water. In the next step, the biopolymers are transformed into randomly oriented carbon structures generating different pores and porosities. Accordingly, the porosity of BC is expected to increase with the ratio of $ZnCl_2$: biomass in its structure; however, its effect is not as significant as phosphoric acid (Khadiran et al. 2014). The formation of new carbonyl and carboxylate ion groups have also been reported which is attributed to the extraction of H element and OH groups from the aromatic rings during the impregnation and heat treatment steps as a result of the dehydration effect of $ZnCl_2$ (Angın et al. 2013). Working on activation of manure-based BC with impregnation of $ZnCl_2$, Xia et al. (Xia et al. 2016) discussed that Zn mainly existed as Zn-OH on the BC surface. The authors found that the adsorption of As(III) on the modified BC (with maximum adsorption capacity of 27.67 mg/g) occurred mainly through ligand exchange of the hydroxyl in Zn-OH to form Zn-O-As(III). They also have compared the effect of $ZnCl_2$ on porosity with NaOH and KOH activation and concluded that numerous pores were densely and evenly distributed across the surface of $ZnCl_2$-activated BC after pyrolysis while NaOH-BC had unsystematic and disordered pore distribution. Generally, most authors have highlighted that properties of the final activated BC strongly depend on $ZnCl_2$ impregnation ratio, activation time and temperature. As per their studies, surface area, total pore and micropore volumes increased when impregnation ratio changed from 1:1 to almost 4:1 (based on the biomass source) (Angın et al. 2013). Some authors have discussed that the increase in surface area and pore volume with impregnation ratio results from the generation of cavities on the surface of $ZnCl_2$ activated BC. The cavities are possibly the spaces previously occupied by the $ZnCl_2$ which was subsequently evaporated during carbonization (Demiral and Demiral 2008, Angın et al. 2013). Hence, aside from the impregnation ratio, increase of temperature (600–900°C) favors the evaporation of more $ZnCl_2$ crystals and generation of more cavities.

2.1.5.1 Application

Among the activating agents, the use of corrosive and hazardous reagents such as zinc chloride is not recommended due to its toxicological and environmental problems, though a few researches have been conducted on this topic because of the activating capabilities of $ZnCl_2$. As an example in terms of wastewater treatment, the adsorption characteristics of $ZnCl_2$-modified bagasse fly ash demonstrated slight improvements in phenol and methylene blue adsorptions (Purnomo et al. 2011). On the other hand, the $ZnCl_2$-ACs have displayed reasonable electrochemical properties with specific capacitances as high as 300–368 F/g (Subramanian et al. 2007, Rufford et al. 2008, 2010). Both improvements in either wastewater treatment or electrochemical properties of $ZnCl_2$-modified BC are attributed to the role of $ZnCl_2$ in improving the porosity of carbonaceous structure. Generally, chemical activation using $ZnCl_2$ is well known to produce ACs with pores wider than 1 nm (Rufford et al. 2010). However, experimental results have demonstrated that $ZnCl_2$ activation produces carbons with superior specific capacitances compared with KOH and NaOH-ACs, though the two latter ones produce carbons with much higher Brunauer-Emmett-Teller (BET) surface areas.

2.2 Basic modification

Similar as in acidic modification, an alkaline modification is conducted by soaking or suspending of either biomass or BC in the desired concentration of an alkaline solution at temperatures between 25°C and 100°C. Soaking and stirring time may last hours or days (mostly 6–24 h) depending on the raw materials used for modification. Alkaline modification produces positive surface charges which in turn assist the adsorption of negatively charged species. Potassium hydroxide (KOH), sodium hydroxide (NaOH) and $ZnCl_2$ are the most common chemical agents used (Cha et al. 2016) for the alkaline activation of char.

2.2.1 KOH

Alkaline metal hydroxides, especially potassium hydroxide which is a prototypical strong base have been frequently used for activation of BC. Production of KOH-activated BC from the KOH-impregnated biomass as precursor follows a series of chemical reactions. The primary reactions include dehydration, cracking, partial polymerization and distortion of biomass (R22) followed by a secondary transformation of the lignocellulosic material to char through

aromatization (R23, R24). Tars and metallic potassium released during this process may spontaneously react with the produced char, resulting in the generation of abundant fine pores and increase the porosity under the high diffusion and pyrolysis action. However, some authors have reported that KOH acts mainly as a dehydrating agent while inhibits tar formation, increasing the carbon yield (Rostamian et al. 2015). As already explained in detail (in Phosphoric acid part), cross-linking and aromatization of the precursor structure caused by activating agents, reduces tar formation and increases carbon yield (Dalai and Azargohar 2007). In parallel, CO_2 reacts with potassium and produces a considerable amount of potassium carbonates and a small amount of metallic potassium (El-Hendawy 2009). The potassium species formed during the activation steps (R25–R27) diffuse into the internal structure of the char, widen existing pores and create new pores (Mao et al. 2014).

$$\text{Ligno.} + KOH \rightarrow \text{Ligno.} - K_2O + H_2O\ (\text{Liquid.}) \quad (22)$$

$$\text{Ligno.} + H_2O \xrightarrow{\Delta} C(\text{Char}) + H_2O + \text{Tar} \quad (23)$$

$$C + H_2O(\text{gas}) \xrightarrow{\Delta} H_2 + CO \quad (24)$$

$$C + H_2O(\text{gas}) \xrightarrow{\Delta} H_2 + CO_2 \quad (25)$$

$$K_2O + H_2 + CO_2 + C \rightarrow C + K_2CO_3 + K \quad (26)$$

$$K_2O + H_2 \rightarrow 2K + H_2O \quad (27)$$

$$K_2O + CO \rightarrow 2K + CO_2 \quad (28)$$

The structural modifications and pore enlargement of BC using alkaline hydroxide activation followed by thermal treatment are associated with the reduction and oxidative modification. These two phenomena are responsible for separation and degradation of graphitic layers resulting in the development of micro and meso porosities. In other words, it is assumed that KOH is reduced to metallic K and carbonate K_2CO_3 during the carbonization/thermal process. The produced carbonate and alkaline metals (in either KOH-impregnated-biomass or BC) are intercalated into the carbon matrix (Lillo-Ródenas et al. 2003), widening and stabilizing the spaces between the carbon atomic layers (Otowa et al. 1997, Lozano-Castelló et al. 2007, El-Hendawy 2009). Simultaneously, the evolution of side reactions between the active intermediates with the carbon surface and release of CO, CO_2, and H_2 are possible. Therefore, a sustained increase in BET surface area and pore volume is expected with increasing the ratio of KOH/char. Generally, KOH activation shifts mean pore diameter to a smaller range and mainly produces narrow/microspores (Wu et al. 2005) (Tseng and Tseng 2005). The carbon oxidization and formation of the corresponding carbonates and metallic potassium can be summarized as below (Hilton et al. 2012, Lado et al. 2017):

$$6KOH + 2C \rightarrow 2K + 2K_2CO_3 + 3H_2 \quad (29)$$

$$3K_2O + 2C + 3H_2O \rightarrow 2K + 3H_2 + 2K_2CO_3 \quad (30)$$

$$2K_2CO_3 + 4C \rightarrow 4K + 6CO \quad (31)$$

$$2K_2CO_3 + C \rightarrow 4K + 3CO_2 \quad (32)$$

Temperature and KOH concentration play the key roles in this process. If activation temperature reaches the boiling point of K (760°C), potassium diffuses into different layers of carbon and forms new pores in the carbon (Rostamian et al. 2015). Therefore, additional porosity might be yielded by further reaction between potassium carbonate and carbon which may increase the carbon burn-off too (Lado et al. 2017). However, KOH modification, even without final thermal treatment, could enhance porosity and specific surface area of BC by significant removal of inorganic matters, clean-up of blocked pores through neutralization reaction between alkali and dust particles and destruction of some micropore structures (Liu et al. 2012, Jin et al. 2014). Aside from temperature, pore size distribution significantly depends on the concentration of the activating agent. Higher concentration usually boosts KOH effect and generates carbon with a higher surface area (Lado et al. 2017). As an instance, the surface area of Corncobs-derived BC activated with KOH/char ratios from 3 to 6 at 780°C is almost 3–4 times higher than those activated with KOH/char ratios from 0.5 to 2 (Tseng and Tseng 2005).

Activation with KOH usually increases alcoholic or phenolic groups (-OH), carboxylic groups (C=O), aromatic groups (C-C), and alkenes (=C-H). However, the surface oxygen groups on the carbon materials decompose upon heating, producing CO and CO_2 at different temperatures. Hence, C contents significantly increase while the quantities of O and H decreased due to the weight loss because of increasing the release of volatile products as a result of intensifying dehydration and elimination reactions (Rostamian et al. 2015). The reduction of O content has also been observed in BCs containing SiO_2 due to its reaction with KOH to form silicate diluted in water through

$2KOH + SiO_2 \rightarrow K_2SiO_3 + H_2O$ (Liu et al. 2012). This result indicates that KOH agent could decrease silica content. Comparison between BC activation with sulfuric acid, phosphoric acid, and potassium hydroxide has shown that KOH activation resulted in a higher quantity of O-containing functional groups and surface area, while H_3PO_4 activation has increased the porosity of BC.

2.2.1.1 Applications

BCs modified with KOH, H_3PO_4 or K_2CO_3 can act as a nutrient source because of the slow release of impregnated potassium or phosphate from the BC surface (Ok et al. 2015). Moreover, since the phenolic hydroxyl groups and carboxylic groups are the major participators in metal adsorption, BCs activated by KOH are efficient agents for removal of toxic metals such as copper (Cu II) (Jin et al. 2016), mercury (Hg), As(V), and Na (Jin et al. 2014, Rostamian et al. 2015). However, although chemical activation using a KOH solution dramatically increases the pore volume and surface area, it may reduce the main exchangeable cations contained in the pyrolytic char (Mg^{2+}, Ca^{2+}, Na^{2+}, and K^{+}) due to their dissolution into the KOH solution. This suggests that ion exchange between heavy metals and the cations which is an important mechanism for the removal of such contaminant may be reduced by KOH activation (Kim et al. 2016). So, the balance between all mechanisms (i.e. ion exchange, co-precipitation, electrostatic surface complexation, physical adsorption, and electrostatic cationic attraction) should be considered for efficient removal of toxic metals.

In contrast, alkali modification significantly improves the adsorption of pesticides by reinforcing the π-π interactions between ring structure of pesticides and graphite-like sheets. As an instance, Liu et al. (Liu et al. 2012) demonstrated that alkali modification (even without post-thermal process) could triplicate the tetracycline adsorption into the BC compared with acidic modification. The theory of π-π interactions between aromatic ring structure (as an electron donor) and graphite-like structure (as a p-acceptor) has been well demonstrated in the literature (Zhu and Pignatello 2005). This mechanism assumes that oxygen functional groups attached to the edge of the carbon basal surface, draw electron density, thus reducing π-π interaction between the aromatic rings and the carbon surface. As per literature, π–π dispersion interaction and the electron donor-acceptor complexes; which contradict each other, are the two most accepted mechanism of phenol adsorption on the carbonaceous structure. An increase of phenol adsorption by KOH-AC demonstrates that π-π dispersion interaction was the dominant mechanism of phenol adsorption as well, which increased with surface alkalinity of the KOH-AC surface (Purnomo et al. 2012).

2.2.2 NaOH

In comparison with KOH activation, chemical activation with NaOH needs lower dosage (weight measurement), is cheaper, less corrosive, and more environmentally friendly (Tseng 2006). Similar to the aforementioned KOH activation, the NaOH impregnated onto BC or biomass reacts with the carbonaceous structure:

$$6NaOH + 2C \rightarrow 2Na + 2Na_2CO_3 + 3H_2 \quad (33)$$

$$3Na_2CO_3 + C \rightarrow 4Na + Na_2O + 4CO_2 \quad (34)$$

$$2Na + CO_2 \rightarrow Na_2O + CO \quad (35)$$

These reactions (Foo and Hameed 2012b) lead to development and enlargement of pores through four phenomena: (i) creation of new pores, (ii) opening of previously inaccessible pores, (iii) widening of the existing pores and (iv) merger of the existing pores due from pore wall breakage (Yang et al. 2010). Compared with alkaline activation with KOH, higher tendency to produce mesoporous carbon has been reported by using NaOH. The results are even more remarkable in case of hydrochars. The average pore diameter of 35.5Å in Rattan stalks-derived hydrochar (Islam et al. 2017), 35.2Å rice husk hydrochar (Ding et al. 2013) and 20.7Å palm date seed hydrochar (Islam et al. 2015) prove this hypothesis. Moreover, NaOH promotes a better chemical activation than KOH due to the non-intercalation mechanism of NaOH compared to intercalation process of KOH (Johannes and Joseph 2015). In other words, Na is smaller than K, so it is intercalated into the carbonaceous structure easily.

The ratio of NaOH/char plays a key role in the activation process and pore development. Excess NaOH molecules over optimum concentration may promote the reduction of Na^{+} cation and OH^{-} anion (Marrakchi et al. 2017). It has been reported that increasing the NaOH:char ratio [to almost 3:1 (Cazetta et al. 2011)] results in a sustained increase in BET surface area and pore volume (Foo and Hameed 2012b). Beyond the optimal concentration, excess NaOH promotes a vigorous gasification reaction, which destroys the carbonaceous structure resulting in a significant reduction of accessible area. In fact, excessive NaOH molecules deposited on the carbon pore wall might

entail catalytic oxidation and decomposition; lowering the carbon yield and adsorption uptake (Lillo-Ródenas et al. 2003, Foo and Hameed 2012b).

$$2Na \xrightarrow{\text{Oxidation}} Na_2 \xrightarrow{\text{Hydration}} NaOH \quad (36)$$

$$4NaOH + C \rightarrow 4Na + CO_2 + 2H_2O \quad (37)$$

In other words, high NaOH concentration induces C-NaOH, C-Na_2CO_3, C-Na_2O, C-Na, C-CO_2, and C-CO reactions facilitating breaking of the C-C and C-O-C bonds, thus reducing carbon yield. Similar results have been reported by rising temperature [to almost 750°C (Byamba-Ochir et al. 2016)]. Working on NaOH activation of chitson flake-based BC, Marrakchi et al. (2017) have reported that additional activation can occur under N_2 flow and high temperature (800°C) by degrading of Na_2CO_3 into Na, CO, and CO_2, which resulted in the development of a more porous structure. As already mentioned, the surface oxygen groups on the carbon materials decompose upon heating, producing CO and CO_2 at different temperatures. Hence, elemental analysis of NaOH activated BC after post-thermal treatment (800°C) shows a large reduction in oxygen content and relatively higher carbon content. Both reduction in O content and increase in C content are intensified due to dehydration reactions as well as the loss of volatile organic products (Roldán et al. 2010). The evolution of CO_2 occurs at low temperatures and is originated by the decomposition of acidic groups, such as carboxylic groups, anhydrides, or lactones. CO evolves at higher temperatures as a consequence of the decomposition of neutral or basic groups, such as phenols, ethers, and carbonyls (Roldán et al. 2010). It has been reported that NaOH increased aromatic carbon fractions and the non-protonated carbon content, indicating the development of a more condensed aromatic structure during the activation. Oxidation of BC structure with KOH differs from those by phosphoric or nitric acid. By using NaOH (without post-thermal treatment), the acidic functional groups (e.g. carboxylic, phenolic groups) are reduced because of their neutralization while the amount of some acidic groups, e.g. lactone group may significantly increase (Li et al. 2017a,b,c,d). Therefore, the total basicity of the treated BC slightly increases, while its acidity reduces. Meanwhile, some other authors reported that the NaOH treatment (without post-thermal process) increases the relative concentrations of hydroxyl groups (the peaks in the range of 3200–3600 cm^{-1}), most probably due to the surface reaction occurring to lactone groups through (Chen and Wu 2004).

(38)

2.2.2.1 Application

The reaction mechanisms of KOH and NaOH with BC are known to be different. KOH intercalates between carbon layers while NaOH reacts with the most energetic sites of the surface (Perrin et al. 2004). However, there are a fewer number of studies on applications of NaOH-modified BC compared with KOH modification. As per literature, high dosage of NaOH turns the micropores into mesopores. Accordingly, determining and applying the suitable ratio between NaOH and BC during activation directly affects the micro-/mesopore volumes and the subsequent adsorption capacity. Accordingly, high dosage of NaOH increases the adsorption of larger molecular adsorbates (dyes: methylene blue, basic brown 1, and acid blue 74) while reduces the adsorption of small molecules (phenols: 2,4-dichlorophenol, 4-chlorophenol, and phenol) (Tseng 2006, Foo and Hameed 2012b, Marrakchi et al. 2017). On the other hand, carbons activated with either KOH and NaOH were successfully employed for electric double-layer capacitance (Ding et al. 2013). NaOH-AC also has a potential to be used as the support material of catalyst in the direct methanol fuel cell (Park et al. 2003) and methane storage (Perrin et al. 2004). In all these, again activating agent concentration and the precursor originality (crystallinity of the carbonaceous precursor) are the key factors to introduce the adequate porosity to the carbon to obtain suitable surface area (Mitani et al. 2004).

3 Sulfonation

Sulfuric acid is a highly corrosive strong mineral acid and shows different properties depending upon its concentration. Sulfuric acid's corrosiveness on other materials is ascribed to its strong acidic nature and, if concentrated, strong dehydrating and oxidizing properties. Sulfuric acid is exerted as a homogeneous catalyst in a wide range of chemical processes which requires efficient methods of separation, and neutralization after the process, generating a remarkable quantity of waste to the environment. Hence, synthesis of sulfonated compounds is a promising technique for the generation of heterogeneous catalysts. Carbonaceous compounds have a potential to be loaded by sulfonic groups (SO_3H) and be used as alternatives to liquid sulfuric acid for the catalysis of chemical reactions.

Activation with sulfuric acid could be followed by a secondary severe thermal process which significantly affects the final results or without it.

3.1 Without final thermal treatment

SO_3H-loaded amorphous carbonaceous compounds such as SO_3H-BC represent a typical class of solid Brønsted acids. As per Brønsted-Lowry theory, a Brønsted acid is any species that is capable of donating a proton $-H^+$. The densities of these acid sites on BC can reach to 2.5 mmol H^+/g. Hence, surface sulfonation, in which sulfonic groups (SO_3H) are added to the BC, has recently gained much attention for the preparation of BC-based solid acids. Sulfonation occurs most rapidly using fuming sulfuric acid (concentrated sulfuric acid that contains 20–30% SO_3), though the reaction can also be progressed in concentrated sulfuric acid, which can generate small quantities of SO_3 (Eq. 39). Sulfur trioxide is a very reactive electrophile and can easily sulfonate aromatic organic compounds to generate sigma complex (Eq. 40). In the next step, a proton is separated from the sigma complex to regain its aromaticity (Eq. 41), and then the oxyanion becomes protonated (Eq. 42), (Figure 13).

$$2H_2SO_4 \leftrightarrow SO_3 + H_3O^+ + HSO_4^- \quad (39)$$

Due to the strong oxidation ability of concentrated sulfuric acid, sulfonation with concentrated sulfuric acid is usually accompanied by oxidation and the peaks assigned to -O-H stretching vibration of hydroxylic groups, -C=O stretching vibration of carbonyl groups, and -C-O stretching vibration are always observed in IR analysis of final functional groups. Comparing these peaks before and after activation reveals that introduction of oxygen-containing functional groups is more often accomplished through the formation of O=C-O group rather than C-O or C=O in BC impregnated with H_2SO_4 after pyrolysis. To reach the carboxylic compound, protons attack the C=C forming the C-OH group. Then C-OH is further oxidized to COOH group (Cainelli and Cardillo 1984). Formation of such graphene carboxylate groups during sulfonation stabilizes the SO_3 amorphous carbon bearing SO_3H groups. Aside from those, some authors reported that sulfonation causes the formation of -SO_3H, O=S=O, and more -O-H groups. IR analysis also shows enhancement in the peaks attributed to C-O/C=N/C-S due to the involvement of C-SO_3H or C-OSO_3H. In some works, reduction in the intensity of the O-C=O peak (at 289.1 eV, 1729 cm^{-1}) confirms its conversion into -O-SO_3H (Liu et al. 2012, Niu et al. 2015, Santos et al. 2015).

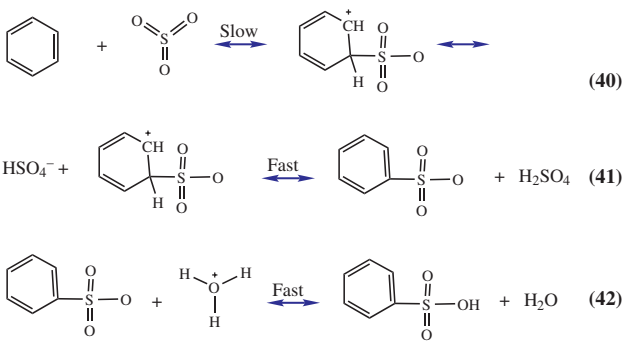

Figure 13: Sulfonation of aromatic rings by using fuming sulfuric acid.

Sulfonation is an exothermic process, hence relatively low temperatures (<150°C) have been applied in most studies and this process normally reduces the BET surface area, pore size, and total pore volume. Applying temperatures higher than 150°C results in a significant reduction in S_{meso}, V_{meso} (surface and pore volume) particularly at a temperature above 250°C while surface acidity (mostly due to phenol and carboxyl) keeps increasing with temperature (Jiang et al. 2003). However, sulfonation under optimal temperature, which depends on the nature of biomass, may slightly increase the S_{BET}, S_{meso}, V_{meso}, and V_{total} at the cost of reduction of micropore surface and volume. The mesoporous volumes and mesoporous areas are reduced after reaching the optimal temperature, though acidity may keep rising (Jiang et al. 2003, González et al. 2017). On the other side, sulfonation of activated BC has a synergistic contribution with activation temperature. It has been reported that if BC is activated at low temperature (~450–500°C), sulfonation could easily decompose the parent polymeric network. While if it is activated at higher carbonization temperatures, the number of C-C bonds in the carbon lattice increases, hence the degree to which the pores collapse, due to the dissociation of the sp^3 based C-C bonding under the decrease of harsh sulfonation conditions (Yu et al. 2011). However, this synergistic effect comes at the cost of the reduction in sulfur content, confirming the reduction of active sites in the final product. This further supports the hypotheses that more heteroatoms evaporate from the carbon rings; larger number of C-H bonds are ruptured with increasing carbonization temperatures. As an example, while increasing the activation temperature of woody-based BC from 450°C to 850°C, the decrease in surface area after sulfonation reduced from 99.1% down to 4.0% at the cost of reduction of total acid density from 2.6 to 0.43 mmol/g (Yu et al. 2011).

3.2 With final thermal treatment

Impregnation of biomass with sulfuric acid before pyrolysis is mainly employed to increase the oxygen-containing functional groups on BC surface. If biomass is impregnated with H_2SO_4 first and then undergoes a pyrolysis process, a significant reduction in the carboxylic group and in contrast a remarkable increase in lactonic groups are observed while the change of phenolic groups depends on H_2SO_4 impregnation ratio. Employing diluted acid results in a slight reduction of the phenolic group but the application of concentrated acid that raises the possibility of over gasification may increase the phenolic quantity too (Karagöz et al. 2008). During this process, the incorporation of sulfuric acid into the interior carbon matrix may retard the formation of tars and promote the introduction of oxygen functionalities which can be represented as follows:

$$2H_2SO_4 + C \rightarrow 2SO_2 + CO_2 + 2H_2O \quad (43)$$

However, the carbon yield obtained via H_2SO_4 activation is relatively low, due to dehydration and gasification effects of H_2SO_4 which has increased the carbon burn off (Guo et al. 2005, Foo and Hameed 2012a).

$$H_2O + [C_nH_xO_y] \rightarrow H_2\uparrow + CO\uparrow + [C_{n-1}H_xO_y] \quad (44)$$

Moreover, wet sulfuric oxidation process resulted in a significant increase of the specific surface area and total pore volume (up to almost 5 times) mainly due the creation and enlargement of pores via carbon gasification (Guo et al. 2005, Foo and Hameed 2012a, Lau et al. 2017). However, high sulfuric acid concentrations may cause over-gasification of parent BC through dehydration of surplus water. In such situation, high destruction effect of H_2SO_4 compared with the other acids converts micropores into meso- and macropores and imposes a great change to the BET and micropore surface areas (Guo and Lua 1999). As an example, over-gasification of the palm-shell precursors when a high concentration of H_2SO_4 (>3 M, or 30%) solution have been used caused a detrimental effect on the BET and micropore surface areas. Hence the surface areas decrease (Guo et al. 2005, Yakout et al. 2015). In most studies, maximum BET and porosity have been reported for H_2SO_4 concentration of up to 3–4 M while its further increment demonstrated a negative effect on the values.

3.2.1 Application

In terms of application, H_2SO_4-treated BCs have a great potential to be used as an alternative route to deal with concentrated H_2SO_4 especially in catalytic applications. By loading sufficient sulfonic groups (SO_3H), these catalysts not only show the activities comparable to the homogeneous H_2SO_4, but also could be recovered and reused several times. One of the best examples which has been frequently addressed in literature includes the development of BC-based catalysts for esterification and transesterification which is the most widely used reactions for biodiesel production (Yu et al. 2011). Esterification reaction by using 20 wt% of this catalyst relative to oleic acid yielded 94% while the use of 1 wt% H_2SO_4 solution showed yield near 98% (Santos et al. 2015).

The graphite-H_2SO_4 intercalation compound is the source for "exfoliated graphite," having a potential use in heat-resisting applications and as an oil absorbent. This topic has not been well addressed in the literature and extension of such studies could be used for future applications of H_2SO_4-BC or H_2SO_4-AC (Kuwata et al. 2009).

4 Amination

Surface amination is among the most common methods to introduce amino groups into BC. Addition of basic amino groups to surface is a promising method for increasing the efficiency of BC in adsorption of carbon dioxide and metal ions. To reach this objective, three different methods can be applied: surface amination through (I) nitration by ammonia, (II) nitration by amino-containing reagents, and (III) combination of nitration and reduction.

The classic surface amination technique usually started with a pre-oxidation process because the graphitic surface of BC is not highly reactive toward NH_3. By doing so, the quantity of carboxylic acid sites in which amination is expected to take place increases. Pre-oxidized BC is then exposed to ammonia (NH_3) at high temperatures (~200°C) for around 2.5 h. According to the mechanisms developed by Jansen and van Bekkum (1994), the reaction of ammonia with carboxylic acids may lead to the generation of amides, lactams, and imides through the following five mechanisms. Dehydration, decarboxylation, or decarbonylation of such functional groups may lead to the formation of pyrroles and pyridines, possibly through nitriles (Jansen and van Bekkum 1994).

Although pre-oxidation and nitration by ammonia can effectively introduce amino groups onto the carbonaceous surface, it suffers from high consumption of energy and releases NH_3 into the environment. Alternatively, chemical modification using some amino-containing reagents is also used for the surface amination of BC. Low molecular

weight amines, including diethanolamine (DEA), methyl diethanolamine (MDEA), and tetraethylenepentamine (TEPA), can accomplish this goal. It has been proved that the -OH, C=O, and especially -COOH groups located on the surfaces of carbonaceous compounds can be chemically transformed into amino groups. In this study, amination of BC with TEPA by using EDC (1-ethyl-3-(3-dimethyl-aminopropyl) carbodiimide) and HOBT (hydroxybenzotriazole) as two activating agents is explained. The procedure is developed based on the results obtained by the current authors in one of the projects aimed at amination of BC for enhancing CO_2 adsorption. Two routes that are considered for grafting tetraethylenepentamine (TEPA) on the two major oxygen functional groups on GO include carboxylic acids and epoxides. Carboxyl group, if not activated, cannot react with the amine in the subsequent step. Whereas reaction of epoxy group and amine occurred without the aid of any activating agents. For last few decades, EDC-benzotriazole-based coupling reaction promoted the amination reaction through activation of carboxyl group very efficiently. Thus, the coupling reaction with EDC-HOBt is the cornerstone for the synthesis of amide. The reaction involves the coupling of amino group to the carboxyl group activated by a coupling agent, e.g. EDC, DCC, etc. EDC is water-soluble which makes it useful in the coupling reaction. Moreover, EDC-benzotriazole produces water soluble by-product. The basic chemistry of amination reaction is depicted in Figure 14.

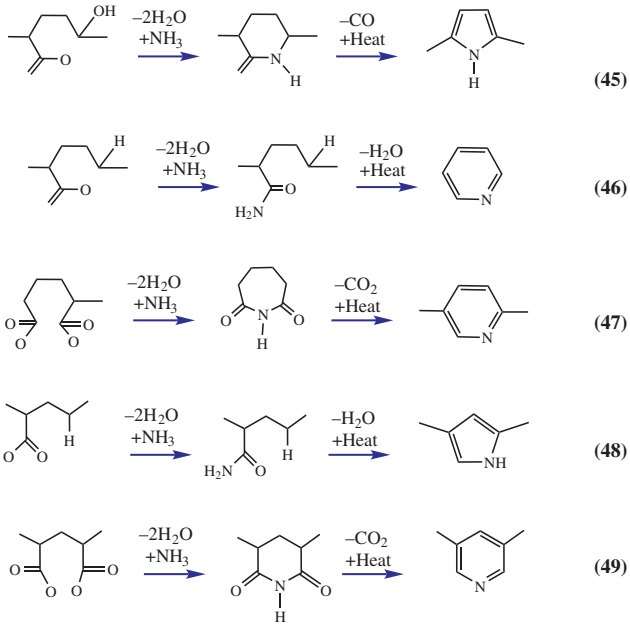

Figure 14: The reaction path of five types of carboxylic acid groups, presumably the most frequently occurring, on the edge of a basal plane; after (i) reaction with ammonia gas, resulting in amide- (46 and 48), imide- (47 and 49), and lactam- (1) groups, and (ii) heat treatment resulting in pyrroles (45 and 48) and pyridines (46, 47, and 49) (Jansen and van Bekkum 1994).

The process starts with the activation of the carboxylic group by attaching it to the EDC to the carboxylic group on BC surface to form O-acylisourea as an intermediate. This intermediate is easily displaced by the nucleophilic attack from amino groups in the reaction mixture which produces amide bond with the original carboxyl group and releases isourea as by-product (Al-Warhi et al. 2012). Another side reaction sometimes could involve O-N migration of the activated carboxyl function forming an N-acyl urea (Al-Warhi et al. 2012). HOBt is the most used additive that prevents urea formation very effectively (Koenig and Geiger 1970). Besides, isolation of products from unreacted reagents can be done by simple filtration since urea is soluble in water which makes the use of EDC and HOBt very significant as coupling reagents (Montalbetti and Falque 2005). Generally, the possibility of attaching the amine group to carboxyl group is higher than epoxide. However, the final product would be a mixture of both. The functionalized GO can then be used as CO_2-capture adsorbents. Separately, the hydroxyl group on GO can also be functionalized by amine for CO_2 capture.

Nitration through the electrophilic aromatic substitution reactions is an effective method for introducing nitrogen-containing functional groups on the condensed aromatic rings of BC (Liang et al. 2008, Yang and Jiang 2014). Electrophilic aromatic substitution can be accomplished by the combination of nitration and reduction. In this process, BC is initially subjected to a nitration process in which nitro groups are introduced to the surface; the nitro groups are then subsequently reduced to amino groups using reducing agents. Amination of BC through the electrophilic aromatic substitution involves a series of reactions (Figure 15) which is started with the generation of nitronium ion, NO_2^+. Nitronium as the active nitrating species in the nitration process is formed by protonation and slow dissociation of nitric acid (Eqs. 53 and 54). Formation of NO_2^+ is considered the rate-controlling step in amination process. This ion then attacks the aromatic C resulting in the formation of Wheland intermediate complex (Eq. 55). Wheland complex (also known as the σ complex or the arenium ion) is a cyclohexadienyl cation that appears as a reactive intermediate in electrophilic aromatic substitution. In the next step, a proton is eliminated from the Wheland complex and is converted to an aromatic compound containing nitrogen (Eq. 56). The nitroaromatic compounds are rapidly reduced by sodium dithionite up to the corresponding anilines (Eq. 57), including a range of possible products (Eq. 58) (Yang and Jiang 2014).

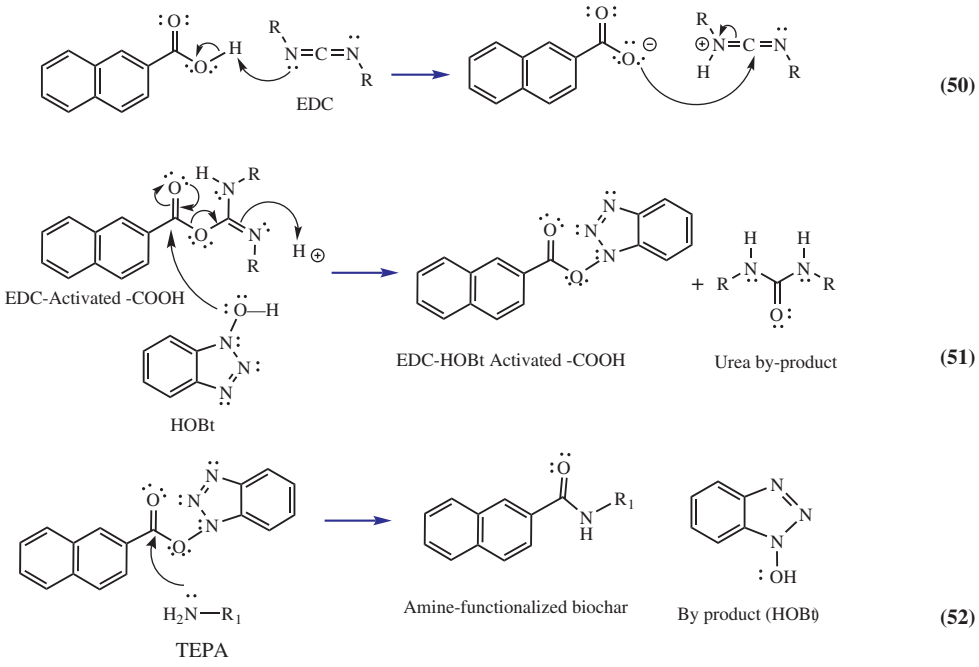

Figure 15: EDC-HOBt coupling reaction and subsequent amine functionalization of biochar, modified based on Chatterjee et al. (2018).

$$HNO_3 + H_2SO_4 \leftrightarrow H_2NO_3^+ + HSO_4^- \quad (53)$$

$$H_2NO_3^+ + H_2SO_4 \xleftrightarrow{\text{Slow}} NO_2^+ + H_3O^+ + HSO_4^- \quad (54)$$

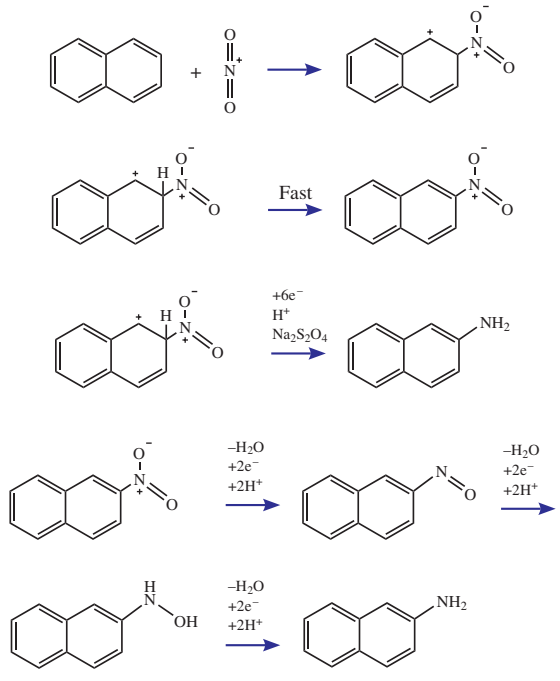

It has been reported that a large quantity of O-containing functional groups are added to the BC by successful grafting of amino groups on the surface. XPS analysis of original and amino-BC revealed the presence of five component peaks, corresponding to (I) graphitic carbon C=C or hydrocarbon C-C which reduced after amino-modification, (II) carbon in phenol, alcohol C-O, C=N, or CNH_2 which increase after amino modification, (III) C=O bonds in carbonyl groups with slight reduction after amino modification, (IV) O=C-O bonds in carboxyl or ester groups with remarkable enhancement after amino-modification, and (V) peaks due to a π-π* transition in aromatic rings which are exactly tripled by amino-modification. As a result, the quantities of carboxyl and phenolic groups significantly increase by using this method of amination caused to increase in surface acidity of BC and a significant reduction in its basicity (Lau et al. 2017).

Surface modification by amination impacts BC's CO_2 adsorption capacity. Hence, most studies have focused on different procedures to increase amination degree. As expected, amination is more effective on BCs with higher BET surface area and hence those synthesized at higher temperatures are more capable for amination and CO_2 capture, though surface area is significantly reduced after amination (Madzaki et al. 2016). Moreover, all amine groups do not behave identically in CO_2 capturing and the adsorption capacity depends on the number of free N atoms in an amine group. As an example, comparing the efficiency of three different amine sources including diethanolamine (DEA), methyl diethanolamine (MDEA),

or tetraethylenepentamine (TEPA) on AC revealed the highest adsorption capacity of 5.63 mmol CO_2/g of AC impregnated with DEA (Gholidoust et al. 2017).

Amine groups efficiently interact with heavy metals and make strong complexes with them due to the high stability constants of the metal complexes, e.g. Cu(II) (Yang and Jiang 2014) and La(III) (Wang et al. 2016a,b). Hence, the amino modification is a promising method for increasing adsorption of metal ions on BC. For example, amino modification of saw dust BC through electrophilic aromatic substitution reactions increased the adsorption capacity of BC toward Cu(II) up to eight-folds of its pristine form (Yang and Jiang 2014).

5 Impregnation

Recent research activities have demonstrated that the nanomaterial can be impregnated into carbon structure. On the other side, nanocrystals of common metal oxides have shown promising potentialities for adsorbing and removing a wide range of toxins from air, acid gases, toxic liquids, chemical warfare agents, etc. (Heroux et al. 2004). Traditionally, BC from most lignocellulosic biomass sources are poor in multivalent metal elements (e.g. calcium, magnesium, ferrous, and aluminum). Hence, nano-metal compounds have gained much attention to producing the intended single- or dual-metallic oxide functionalized BCs for efficient anionic pollutants removal (Jung et al. 2016, Li et al. 2016a,b). The procedure for homogeneous metal impregnation is normally accomplished using a solution containing metal salts (e.g. $AlCl_3$, $MgCl_2$, $LaCl_3$, or $FeCl_3$) or metal oxides (MgO, MnO, CaO, ZnO, TiO_2, and Fe_2O_3) before or after pyrolysis which can also be followed by thermal treatment (Ahmed et al. 2016, Jung et al. 2016). Dip-coating is a well-known approach for the synthesis of nanomaterial-impregnated BC. In dip-coating, BC is added into suspensions of nanomaterials, stirred for the desired duration, then filtered and dried. Another procedure for impregnating the nanomaterials on BC is the self-assembly method, in which the suspension is allowed to age at a certain temperature without stirring. Multiple times of rinsing with deionized water are usually needed to remove the loosely bound nanomaterials for ensuring stability and purity of modified BCs (Ok et al. 2015).

5.1 Impregnation with magnesium oxide

MgO is a typical alkaline earth metal oxide with excellent adsorption capacity, environmentally friendly, and naturally abundant. A typical pathway for synthesis of the mesoporous carbon stabilized MgO can be started by loading of $MgCl_2$ on biomass. The $MgCl_2$-preloaded biomass is then subjected to the pyrolysis in which $MgCl_2 \cdot 6H_2O$ is dehydrated and decomposed to MgO at high temperatures (Liu et al. 2013a).

$$MgCl_2 \cdot 6H_2O \rightarrow MgCl_2 \cdot 2H_2O + 4H_2O\uparrow \quad (59)$$

$$MgCl_2 \cdot 2H_2O \rightarrow Mg(OH)Cl + H_2O\uparrow + HCl\uparrow \quad (60)$$

$$Mg(OH)Cl \rightarrow MgO + HCl\uparrow \quad (61)$$

As per literatures, magnesium NPs do not significantly affect the structural formation of organic functional groups (Fang et al. 2014a,b), but MgO particles in the BC matrix can strongly bind anions in aqueous solution through mono-, bi-, and tri-nuclear complexions. These findings indicate that cationic modification using MgO increases the ability of BC to remove anionic nutrients from aqueous solutions (Li et al. 2017a,b,c,d). As an example, Zhang et al. (2012) produced porous MgO-BC nanocomposites from five various types of biomass feedstocks. These nanocomposites demonstrated exceptional adsorption ability to anions and hence were used for phosphate and nitrate adsorption. Fang et al. (2015a,b) added Ca to Mg-loaded BC which significantly increased the phosphorus adsorption and its recovery. The synthesized Ca-Mg/BC was rich in the organic functional groups of hydroxyl, carboxyl, carbonyl, and methoxyl, as well as the NPs of CaO and MgO (Fang et al. 2015a,b). In a corresponding study by the same group, BC impregnated with aluminum (Al) was found to effectively remove arsenic, methylene blue, and phosphate from aqueous solutions (Zhang and Gao 2013). Accordingly, in the last effort, Zhang et al. (2013) used $MgCl_2$ and $AlCl_3$ solutions to prepare an AL-Mg/BC and could reach the maximum phosphate removal of 410 mg/g. Though, nano-sized MgO particles loaded BC have superior adsorption capability to phosphate (Jung and Ahn 2016), its synthesis by following the procedure presented in Eq. (59–60) is quite slow. Hence, Jung and Ahn (2016) applied an electrochemical reaction by using $MgCl_2$ as an electrolyte creating strong oxidants (i.e. HOCl and OCl^-) in solution. They were able to synthesize a porosity-enhanced BC containing MgO NPs within only few minutes and achieved the phosphate adsorption as high as 620 mg/g.

MgO is a desirable and effective adsorbent for the removal of heavy metals from aquatic environment too. However, the problem associated with MgO-loaded compounds is the agglomeration of nano-sized MgO on carrier

surfaces that suppresses its efficiency. If this problem is eliminated, MgO-BC can exhibit a high capacity and fast adsorption of heavy metals. To reach this objective, Ling et al. (2017) introduced $MgCl_2$ into an N-enriching hydrophyte biomass and successfully stabilized (MgO) NPs on the N-doped BC and achieved a large Pb adsorption capacity (893 mg/g) in a very short equilibrium time (<10 min).

As per literature, MgO material can adsorb CO_2 at a relatively low temperature and because of abundancy, it is economically attractive. However, MgO-BCs have exhibited relatively poor CO_2 adsorption capacity (<1 mmol/g). Hence, a number of researchers have focused on improving their CO_2 adsorption capacity (Shahkarami et al. 2016). The CO_2 capture sites of the MgO are mainly the basic O^{2-} in the O^{2-}-Mg^{2+} bonds, and the basic strength of the O^{2-} depends on its coordination. The O^{2-} ions located in the planes of the crystal surfaces often have weaker basicity than those at the corners and edges. Compared with the bulk MgO materials, the nano-sized MgO particles, due to their small size, have more corners and edges per weight, and thus possess more active sites (basic O^{2-}) for CO_2 capture. Liu et al. (2013a) synthesized a mesoporous carbon-stabilized MgO NP through fast pyrolysis of the $MgCl_2$-loaded waste biomass which presented an excellent performance in the CO_2 capture process with the maximum capacity of 5.45 mmol g^{-1}. Moreover, sintering of agglomerated MgO particles during the high-temperature regeneration process reduces the cyclic stability of MgO-loaded BC. Zhang et al. (2016a,b) have discussed that using the confinement effect of pores to prepare highly dispersed and relative independent MgO NPs may delay the agglomeration of MgO and thus increase the cyclic stability of MgO-loaded structures. Unfortunately, this problem has not been well addressed in the literature and therefore could be a suitable topic for future research.

5.2 Impregnation with manganese oxide

The MnO_2-BC composite is usually fabricated via simple and cost-effective redox process. The self-controlled reaction between the carbonaceous structure of BC and potassium permanganate ($KMnO_4$) under neutral pH conditions results in the formation of a homogeneous deposition of nano-sized MnO_2 particles on BC surface. The reaction between carbon and $KMnO_4$ is as follows (Zhao et al. 2012):

$$4MnO_4^- + 3C + H_2O \rightarrow 4MnO_2 + CO_3^{2-} + 2HCO_3^- \quad (62)$$

Manganese (Mn) is present in more than 30 different oxide minerals which are commonly found in terrestrial environments and soil. Among them, "Birnessite" is one of the most abundant while "Manganosite" is a rare mineral composed of MnO. In terms of BC synthesis, using $KMnO_4$ results in fabrication of birnessite oxide while using $MnCl_2 \cdot 4H_2O$ solution leads to the formation of manganosite oxides (Wang et al. 2015a,b). In this topic research, except the work presented in Wang et al. (2015a,b), all researchers have used $KMnO_4$. Both mineral structures of MnO have a high potential for Pb(II) (Wang et al. 2015a,b), Cd(II) (Liang et al. 2017), As(III), and As(V) (Wang et al. 2015a,b) sorption which is associated with internal reactive sites. Hence, MnO_2-loaded BC has been frequently tested in adsorption of these heavy metals. Birnessite has a high oxidization potential and high adsorption capacity toward arsenite (As(III)) and arsenate (As(V)). In fact, MnO-modified BC adsorbs and partially converts As(III) to its less toxic form, As(V)) (Yu et al. 2015). The sorption of As(V) by birnessite gradually decreases between pH 2 and 10, proving the surface complexation interactions between MnO and As(V) which occurs at the proper ambient pH. In this interaction, surface hydroxyl group on MnO-BC is displaced by the oxygen moiety of As(V), generating an inner-sphere complex. Hence when impregnated, BC/birnessite (B-BC) shows enhanced sorption of As(V) (0.91 mg/g) and Pb(II) (47.05 mg/g), in comparison to the pristine BC (As(V): 0.20 and Pb(II): 2.35 mg/g) and BC/manganosite (M-BC) (As(V): 0.59 and Pb(II): 4.91 mg/g) (Wang et al. 2015a,b). Adsorption of Pb(II) by B-BC is significantly higher than As(V). This is due to either diffusion into birnessite interlayers, by replacing cations located above or below the vacancy sites of birnessite, or by coordination to vacancy sites of hexagonal birnessite surface structure (Wang et al. 2015a,b). However, the method of synthesis remarkably affects the adsorption capacity of B-BC. As an example, Wang et al. (2016a,b) synthesized Ni-Mn oxides BC through two methods, pyrolysis of Ni-Mn modified feedstock (NMMF) and Ni-Mn modification of pyrolysed BC (NMMB). The results indicated that maximum As(V) sorption by NMMB (with the dominant mechanism of electrostatic attraction) was about 12 times of NMMF sorption (with the dominant mechanism of anion exchange and surface complexation). Using similar method of synthesis, Liang et al. (2017) used the $KMnO_4$ as a strong oxidizing agent to promote the incorporation while they also added Mn(II) acetate tetrahydrate solution under continuous stirring to control the level of loading, producing dark brown precipitation of MnO_2 in the suspension according to:

$$3Mn^{2+} + 2MnO_4^- + 2H_2O \rightarrow 5MnO_2 \downarrow + 4H^+ \quad (63)$$

The synthesized MnO_2-BC demonstrated superior adsorption performance (maximum capacity for Pb

268.0 mg/g and Cd 45.8 mg/g) compared with the pristine BC (Pb 127.75 and Cd 14.41 mg/g) (Liang et al. 2017).

Manganese oxide has also gained wide attention in degradation of many gaseous pollutants, the transformation of alcohols to aldehydes or ketones, as a catalyst for CO and benzene oxidation, and also for HCHO removal from indoor air (Li et al. 2016a,b). HCHO would be continuously oxidized by the layered MnOx at room temperature provided by timely compensation of the consumed hydroxyl groups on the surface of MnOx in the air. To overcome the drawbacks of powder MnOx in the practical application, some authors have deposited MnOx on solid substrates such as AC nanofiber (Miyawaki et al. 2012) or cellulose fibers (Zhou et al. 2011). The MnOx/AC materials have shown a high activity for HCHO removal at both high (Zhou et al. 2011) and room temperature (Li et al. 2016a,b) (depends on the method of synthesis) and thermal regenerability at temperatures as low as 60°C (Li et al. 2016a,b). This area opens a new topic that needed to be investigated by employing BC as solid substrates.

Manganese oxide-based compounds can also serve in energy storage applications due to their specific capacitance of 1370 F/g, though the specific capacitance of MnO_2-based supercapacitor that depends on the particle size to a high extent. In addition, MnO_2 suffers from poor cyclic instability and electrical conductivity. In response to these weaknesses, MnO_2 NPs incorporated with 2- or 1-dimensional nanomaterials were fabricated. The sp^2-carbon-rich carbon dots (CDs) exhibited a strong interaction with graphene through π-π, stacking for self-immobilizing on graphene. Meanwhile, MnOx can be grown *in situ* on CDGs at a mild reaction temperature (75°C) under which CDs on graphene undergo sacrificial oxidation for the formation of nano-sized MnOx, while the graphene's graphitic carbons are protected. As per these information, Unnikrishnan et al. (2016) synthesized a supercapacitor with the specific capacitance of ~280 F/g by using carbon dots as a dispersing agent of graphene as well as a reducing agent of $KMnO_4$. In a comparative study, Zhao et al. (2012) deposited MnO_2 on expanded graphite oxide which yielded a specific capacitance of 256 F/g. The maximum specific capacitance of 357 F/g was reported for a supercapacitor synthesized by coating manganese oxide onto a network composed of single-walled carbon nanotubes (Wang et al. 2011). Since BC is made of different layers of graphene oxide, a similar outcome is expected if graphene is substituted with BC. However, there are very scarce studies on this topic especially by using BC. As an instance, Wan et al. (2016) used wood-derived BC to support sheet-like nano-MnO_2 via *in situ* redox reaction and reported the moderate specific capacitance of 101 F/g. More research related to this topic is required.

5.3 Impregnation with calcium oxide

Calcium compounds tend to be adsorbed to the surface of BC, thereby raising pH, and providing a source of calcium oxide on BC surface. Synthesis of Ca- or CaO-loaded BC usually includes impregnation of biomass with calcite ($CaCO_3$), calcium dihydrogen phosphate [Ca-$(H_2PO_4)_2$], or any other calcium-contained compound such as $CaMg(CO_3)_2$, followed by pyrolysis process (Przepiórski et al. 2013, Li et al. 2014). By doing so, Ca^{2+} ions are adsorbed onto graphene oxide nanoclusters of BC and dissolved in the carbon-rich regions. Archanjo et al. (2014) modeled and investigated six different mechanisms of this phenomenon (Figure 16).

As per their work, the basal graphene plane is an ideal location of Ca^{2+} adsorption on pristine graphene. The interaction between the Ca^{2+} cation and the π-electrons of the basal plane with the adsorption energy of –121 kcal/mol allows binding calcium ions strongly to the carbon atom (Ca-C). The adsorption of Ca^{2+} with epoxide groups, with the adsorption energy of –147 kcal/mol, forms a "bridge" between two neighboring carbon atoms. However, Ca^{2+} breaks apart one of the O-C bonds and generates one strong

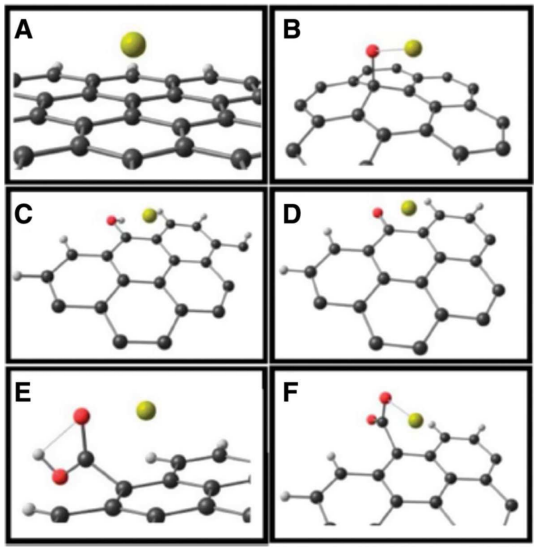

Figure 16: Atomic geometries for the different structures considered Ca^{2+} adsorption on pristine graphene: (A) Ca-C sp2, (B) Ca – epoxide, (C) Ca – hydroxyl (edge), (D) Ca – carbonyl, (E) Ca – carboxyl, and (F) Ca – carboxylate. Carbon: black, hydrogen: white, oxygen: red, and calcium: yellow (Archanjo et al. 2014), with copyright license, American Chemical Society.

Ca-O species. In the other possible interaction, Ca^{2+} cation ion strongly binds with a hydroxyl group in the basal plane, removing it from the carbonaceous structure. As per the computational analysis, two OH groups are removed from the surface each by single Ca^{2+} and are converted to $Ca(OH)_2$. However, if Ca^{2+} ions are adsorbed by hydroxyl group of the crystallite edge (with adsorption energy of –125 kcal/mol), Ca-O is formed without removing the OH group. A similar procedure with almost the same adsorption energy can be accomplished by interaction of Ca^{2+} with a carbonyl group at the edge, generating another Ca-O. Adsorption of Ca^{2+} by carboxyl groups at the graphene nanocluster edge (with the adsorption energy of –146 kcal/mol) is another possibility. However, its stability depends on the pH of the media. The energy of adsorption may reach up to –292 kcal/mol in a stable interaction (Archanjo et al. 2014).

Studies have shown that the exogenous presence of calcium elements significantly enhances the carbon retention and stability of BC. Li et al. (2014) observed the carbon loss of 16.0 and 7.78% in both $CaCO_3$-BC and $Ca(H_2PO_4)_2$-BC, compared with 18.8% in raw BC. This is probably due to the reduction of dissolved organic carbon content by 39.8% and increment of aromatic C by about 33.1% in the modified samples.

Some biomasses (for instance: crab shell) contain a high quantity (15.8%) of Ca (Dai et al. 2017). Li et al. (Dai et al. 2017) used crab shell-based BC and could remove 80 mg P/l phosphate solution. Agrafioti et al. have reported that the BCs impregnated with either Ca^{2+} or Fe^{3+} ions demonstrated a significant improvement in the removal of As(V), while the corresponding removal rate for the samples impregnated with Fe^0 was lower. In terms of the Cr(VI) removal, adsorption rates were not as high as the As(V) ones, except sample engineered with Fe^{3+} (Agrafioti et al. 2014).

Calcium compounds in the forms of neat, mixed, loaded, or supported CaO are promising catalysts for transesterification of triglycerides (oily feedstocks) for biodiesel production. Some researchers have recently demonstrated that calcium carbonate content in palm kernel shell can be used as CaO-based catalyst (Kostić et al. 2016). However, CaO-based catalysts suffer from leaching of CaO during the reaction, which not only inversely affects the reusability of the catalyst, but also contaminates the final products.

Calcium oxide-based sorbents have also shown promising potentials for the capture of carbon dioxide. The kinetics of reactions $Ca + CO_2 \rightarrow CaO + CO$ and $CaO + CO_2 \rightarrow CaCO_3$ at ambient conditions (Plane and Rollason 2001, Broadley et al. 2008) and at high temperatures (Lu et al. 2006) have been widely studied in the literature. Using computational analysis, Cazorla et al. (2011) claimed that Ca-decorated graphene and nanotubes possess unusual large CO_2 uptake capacities (~400–600 mg CO_2/g sorbent). However, most practical studies in this area have obtained much lower adsorption capacities even by using AC rather than BC. As an example, Przepiórski et al. (2013) prepared an AC loaded with CaO and MgO through a one-step process from mixtures of poly (ethylene terephthalate) and dolomite mineral. The obtained hybrid materials removed 12.3 mg CO_2/g air at 70°C.

And the last but not the least proved the advantage of synthesis of Ca-loaded BC is in gasification. Biomass gasification process suffers from several drawbacks due to a high moisture content of biomass as well as its low mass and energy densities, which imposes the use of dryer and high-temperature (700–1000°C) gasifiers. Hence, BC with high heating value and low moisture retention provides a more attractive option for gasification. Moreover, carbon gasification yields a higher efficiency in the hydrothermal medium compared with that in the thermal medium. Addition of K_2CO_3 or KOH catalysts can further enhance the efficiency of the process. Studies over this area show that gasification can be remarkably enhanced if a small amount of $Ca(OH)_2$ is added to biomass prior to producing the BC. As an example with the use of $Ca(OH)_2$ and K_2CO_3 during hydrothermal carbonization and hydrothermal gasification respectively, Ramsurn et al. (2011) could enhance the yield of hydrothermal gasification from 43.8% to 75% in short reaction time at 600°C. The authors discussed that $Ca(OH)_2$ mitigates the catalyst deactivation by preventing the reaction between K_2CO_3 and the minerals in biomass structure. In other words, it alters the chemical properties of the inherent minerals in biomass. It is also believed that calcium compounds facilitate the formation of oxygen complexes on carbon, hence promoting the carbon gasification reaction (Zhang et al. 1989).

5.4 Impregnation with Cu ions

Numerous studies have demonstrated that metallic catalyst-modified BC can increase the selectivity and capacity of pollutant removal. However, in terms of copper, most studies have focused on removal of copper ions from wastewater (Hamid et al. 2014) rather than improving the performance of BC by adding copper ions into BC structure. Copper-loaded BC can be fabricated by impregnation of either biomass or BC with hydrated copper(II) nitrate,

copper(II) chloride, and copper (II) acetate which produce Cu(II) ions. The following reactions have been suggested for these processes:

$$(\text{-RO}^{+}\text{H}_2) + \text{Cu}^{2+} \rightarrow (\text{RO})\text{Cu} + 2\text{H}^{+} \quad (64)$$

$$n\text{R-COOH} + \text{Cu}^{2+} \rightarrow (\text{R-COO})_n\text{Cu} + n\text{H}^{+} \quad (65)$$

However, aside from Cu(II) cations, copper can exist in its hydroxide form in water at pH 6 and may interact with the hydroxyl group on BC surface through the following reaction (Hamid et al. 2014).

$$(\text{-RO}^{+}\text{H}_2) + \text{Cu(OH)}^{+} \rightarrow (\text{-RO})\text{CuOH} + 2\text{H}^{+} \quad (66)$$

XRD analysis shows that fraction of Cu(II) atoms interacts with hydroxyl, and carboxylate functional groups on the surface of BC and hence this process may also contribute in introducing some more oxygen-containing functional groups onto BC. Following the aforementioned procedure, Liu et al. synthesized the Cu-BC absorbent through calcination of peanut shell biomass and then impregnation with copper nitrate. FTIR analysis of the produced Cu-BC indicated the formation of Cu-O bond, Cu-N bond (interactions between Cu(II) and the -NH_2 groups on BC surface and chelation of Cu(II) with -OH group. The authors reported that Cu-BC has exhibited an almost double amount of sorption of doxycycline hydrochloride compared to that of the unmodified BC through the electrostatic interaction and complexation (Liu et al. 2017).

In terms of application, CuO-modified BC has shown catalytic applications, such as in catalytic wet air oxidation for wastewater treatment. However, the stability of catalyst and leaching of active sites are the key factors in systems including heterogeneous catalysts. Hence, Álvarez et al. (Álvarez et al. 2002a,b) focused on the leaching of copper from 5% CuO-loaded AC in their work on wet air oxidation of phenol. Except for the first experiment which was accomplished using fresh catalyst, signs of copper leaching were observed when the catalyst was reused in consecutive experiments. However, the authors concluded that the leaching of the active substance from CuO-modified BC was much lower than in case of commercial Cu-Zn/Al_2O_3. In another work, Cho et al. (2017) synthesized nitrogen-doped Cu-BC via pyrolysis of glucose in the presence of copper and melamine and used it as a catalyst in the reduction of p-nitrophenol by NaBH_4. These authors have also detected three characteristic peaks for pure metallic copper and four characteristic peaks for cuprous oxide (Cu_2O). They concluded that this improvement in BC greatly influenced the reduction kinetics, increasing linearly reaction rate constants.

5.5 Impregnation with nickel oxide

Ni-loaded BC can be obtained by wet-impregnation of biomass prior to pyrolysis of BC in Ni(II)nitrate solution, $\text{Ni(NO}_3)_2$, followed by pyrolysis or a thermal treatment, respectively. In general, metal adsorption is mainly due to ion exchange with mineral cations naturally present in biomass and in terms of Ni, it is adsorbed onto BC most probably through the combination of Ni^{2+} and CO_3^{2-} the latter being an inherent anion in BC. Complexation of Ni with O-containing groups is the other possible mechanism and since PO_4^{3-} is another anion available in BC, the formation of $\text{Ni}_3(\text{PO}_4)_2$ is also possible.

$$5\text{Ni(NO}_3)_2 + 24\text{H}_2\text{O} \rightarrow \text{Ni}^{2+} + 4[\text{Ni(H}_2\text{O)}_6]^{2+} + 10\text{NO}_3^{-} \quad (67)$$

$$\text{Ni}^{2+} + \text{CO}_3^{2-} \rightarrow \text{NiCO}_3 \downarrow \quad (68)$$

$$2\text{-C-O}^{-} + \text{Ni}^{2+} \rightarrow (\text{-C-O})_2\text{Ni} \quad (69)$$

$$2\text{-C-OO}^{-} + \text{Ni}^{2+} \rightarrow (\text{-C-OO})_2\text{Ni} \quad (70)$$

Sorbed Ni can then be transformed into Ni oxide by a thermal treatment through the following reactions:

$$[\text{Ni(H}_2\text{O)}_6]^{2+} \rightarrow \text{Ni(OH)}_2 + 2\text{H}_3\text{O}^{+} + 2\text{H}_2\text{O} \quad (71)$$

$$\text{Ni(OH)}_2 \rightarrow \text{NiO} + \text{H}_2\text{O} \quad (72)$$

$$\text{NiCO}_3 \rightarrow \text{NiO} + \text{CO}_2 \uparrow \quad (73)$$

$$2(\text{-C-O})_2\text{Ni} + \text{O}_2 \rightarrow 2\text{NiO} + 2\text{CO}_2 \uparrow \quad (74)$$

$$2(\text{-C-OO})_2\text{Ni} + \text{O}_2 \rightarrow 2\text{NiO} + 4\text{CO}_2 \uparrow \quad (75)$$

$$\text{Ni}^{2+} + 2\text{H}_2\text{O} - \text{e} \rightarrow \text{NiOOH} + 3\text{H}^{+} \quad (76)$$

Ni-impregnated biomass catalyzes cracking and reactions of volatile compounds in the lignocellulosic matrix, leading to significant changes in the yields of char and other products. Knowing this, Shen et al. (2014) proposed an integrated approach of *in situ* tar and syngas conversion technology for biomass pyrolysis/gasification by the pretreatment of nickel impregnation. The authors discussed that Ni-based catalyst not only converted the removed tar into extra gases with the efficiency of 96.9% by thermochemical reactions but it also enhanced the pyrolysis

efficiency and restrained the formation of condensable tar due to polymerization.

Among different metal oxides, NiO has gained much attention due to its high theoretical specific capacitance (2584 F/g) and good redox activity. The Ni-oxide particles in the electrochemistry system undergo the following reaction to donate or accept electrons:

$$NiO + OH^- \rightarrow NiOOH + e^- \quad (77)$$

Wang et al. (2017a,b) synthesized two different BCs derived from dairy manure and sewage sludge and soaked them into $Ni(NO_3)_2$ solution to syntheses the Ni-loaded BC. The authors concluded that compared with the original BC supercapacitors, the Ni-loaded BC slightly increased the capacitance. However, the capacitance increased by over 2 times after microwave treatment which was mainly attributed to the conversion of Ni into NiO and NiOOH as evidenced by X-ray diffraction.

5.6 Impregnation with zinc oxide

Zinc oxide because of its unique structure and electronic properties is considered as a powerful adsorbent. Moreover, fabrication of nano-sized ZnO particles and impregnation of them on other structures are quite easy. ZnO is a direct band gap semiconductor (3.36 eV at room temperature), so it is a potential compound in ultraviolet emitting devices with a particular focus on photo-degradation processes (Changsuphan et al. 2012). Zinc oxide is extremely stable, does not degrade from sun exposure, and is well suited for water-resistant sunblock. Furthermore, zinc oxide exhibits anti-bacterial properties and is used in pharmaceutical applications. Nano-zinc oxide powders are used in sunscreens and sun blockers, lipsticks, anti-bacterial lotions, rubber emulsions, UV stabilizer in plastics, as a catalyst in the chemical industry, and as a food additive.

ZnO impregnation can be easily accomplished by suspending either BC or AC in ZnO solution followed by a mild thermal treatment (250–350°C). It has been reported that due to the homogenous coating of the ZnO-np onto the AC or BC, this process generates products with a uniform surface (Nourmoradi et al. 2015). It also increases the specific surface area due to the enlargement of mesopore volume and their surface area, while a detrimental effect was observed in micropore volumes (Kikuchi et al. 2006). The other important effect of zinc oxide is dissociation of hydrogen from water in a heterogeneous manner and creation of hydroxyl groups. Surface hydroxyl groups on the zinc oxide can then be formed on AC by coming into contact with water. Therefore, zinc oxide can increase the adsorption capacity of carbon compounds toward heavy metals by creating hydroxyl groups (Kikuchi et al. 2006). Kikuchi et al. studied the loading of ZnO on AC and observed the maximum adsorption capacity of 0.37 mmol/g which was almost equal to the amounts of zinc oxide loaded (0.35 mmol/g), suggesting the mono-layer spreading of zinc oxide onto the AC surface. Gan et al. (2015) have worked on a new synthesis method by impregnating of biomass with zinc nitrate solution followed by pyrolysis in a tube furnace up to 450°C. They used this process for removing Cr(VI) and could reach the maximum sorption capacity of 102.66 mg g^{-1}. Various studies have mainly emphasized on the role of ZnO in increasing the hydroxyl and carboxyl groups as the main functional groups for removal of heavy metals.

ZnO-AC and ZnO-BC have been successfully tested in treating different dye-containing wastewaters such as methylene blue, acid orange 7 (Nourmoradi et al. 2015), methylene green (Ghaedi et al. 2014), and p-nitrophenol (Wang et al. 2017a,b). Ghaedi et al. (2014) reported that AC-loaded ZnO nanorods not only has higher capacity compared with silver-loaded AC in adsorbing methylene green (200 vs. 166.7 mg g^{-1}), but the associated process is also faster.

5.7 Magnetization

Although BC has exhibited promising sorption ability, separation of BC powder from aqueous solutions is difficult and limits its practical application at industrial scale. Removal of such small particles usually imposes a separation step (e.g. filtration or centrifugation) and adds the subsequent extra cost to the treatment process. Inducing magnetic particles into BC provides a promising solution to this obstacle (Harikishore Kumar Reddy and Lee 2014). Magnetically modified BCs form ferromagnetic particles and can be easily separated from the aqueous solution by using an external magnet. Reuse of magnetic BC is technically and economically feasible since the regeneration process is simple and can be carried out *in situ* within a short time (Wang et al. 2015a,b). In short, magnetic BC has been proved to provide effective adsorptivity, fast separation, easy recycling (Han et al. 2016), and is applicable for removing heavy metals, dye, and oil from aqueous water (Wang et al. 2014). The magnetization of BC is usually accomplished by fusing an iron oxide phase to the carbonaceous structure of BC. There are 11 known iron oxides including the oxides of Fe^{II} (FeO) and Fe^{III} (different species

of Fe_2O_3 such as α-Fe_2O_3, β-Fe_2O_3, γ-Fe_2O_3, and ε-Fe_2O_3) and mixed oxides of Fe^{II} and Fe^{III} (Fe_xO_y, e.g. Fe_3O_4). The other oxygen-containing compounds of iron include hydroxides and oxy-hydroxides. However, all of these iron oxides do not have ferromagnetic properties. As an example, γ-Fe_2O_3 and Fe_3O_4 (known as magnetite) are magnetic iron oxides while α-Fe_2O_3 (known as hematite) and iron hydroxides ($Fe(OH)_2$ and $Fe(OH)_3$) do not have magnetic properties. The presence of non-magnetic iron oxides/hydroxides in BC structure reduces the magnetic saturation of the magnetic adsorbent, making the recovery process more difficult (Reguyal et al. 2017). Nevertheless, unwanted, non-magnetic $Fe_x(OH)_y$, $Fe(OH)_2$ and $Fe(OH)_3$ sometimes are being formed in magnetization of BC. It has been reported that oxidative hydrolysis of $FeCl_2$ under alkaline media can introduce the most magnetic Fe_xO_y, -Fe_3O_4, on BC and controls or in fact prevents the formation of non-magnetic compounds (Reguyal et al. 2017). Aside from such iron-oxide loaded BC, the other magnetic particles can also be employed to achieve magnetic properties. As an example, BC-modified with spinel ferrite with the general formula of AFe_2O_4 (A = Mn, Zn, Ni, Co, Fe, etc.) demonstrated satisfying structural stability, adsorption performance, and ferromagnetic property because of the variable valence of iron (Harikishore Kumar Reddy and Lee 2014). Iron-based nano-scale bimetallic particles are the other compounds that can be used for BC modification. As an example, Ni/Fe demonstrated remarkably high dechlorination effect towards 1,1,1-trichloroethane (TCA) and the adsorption increased as the BC to Ni/Fe mass ratio increased from 0 to 1.0 (Li et al. 2017a,b,c,d). Successful methods in synthesizing magnetic BC are categorized into three major groups: direct pyrolysis of metal salt-loaded biomass (Reddy et al. 2014, Zhu et al. 2014), liquid-phase co-precipitation of ferrous(Fe^{2+})/ferric(Fe^{3+}) salts (Ngarmkam et al. 2011, Mohan et al. 2015), and reduction of ferrous salt by borohydride (Devi and Saroha 2015). Magnetization by chemical co-precipitation has been widely used for the introduction of Fe_3O4/γ-Fe_2O_3 into BC structure. In this method, a combined mixture of Fe^{2+} and Fe^{3+} ions are used in an alkaline solution, such as ammonium hydroxide, sodium hydroxide, or potassium hydroxide. Co-precipitation is usually performed under an inert atmosphere (Ar or N_2) using degassed solutions to avoid uncontrollable oxidation of Fe^{2+} into Fe^{3+} (Mascolo et al. 2013). However, co-precipitation is a complex process of magnetization since it is generally applied after the completion of pyrolysis. Moreover, decrease or block of adsorbent pores has been observed in magnetic BC synthesized through this method, making some surfaces unavailable for adsorption (Noraini et al. 2016, Shan et al. 2016).

Reduction of iron salts [$FeCl_3 \cdot 6H_2O$, $Fe_2(SO_4)_3 \cdot 5H_2O$, or $FeCl_2 \cdot 4H_2O$)] by a reductant such as sodium borohydride is another method in BC magnetization. This process is physically simple, but chemically follows a complex reaction:

For Fe(III) compounds:

$$Fe(H_2O)_6^{3+} + 3BH_4^- + 3H_2O \rightarrow Fe(s) + 3B(OH)_3 + 10.5H_2(g) \quad (78)$$

For Fe(II) compounds:

$$Fe(H_2O)_6 + 2BH_4 \rightarrow Fe(s) + 2B(OH)_3 + 7H_2(g) \quad (79)$$

In this process, sodium borohydride is normally used in high excess with respect to the ferrous or ferric ions to achieve a rapid and uniform growth of iron crystals. Reduction of ferrous salt is sensitive to a variety of parameters, such as the concentration and addition rate of borohydride (which alter the composition of the reaction product) and pH (which affect the particle size) (Bundschuh et al. 2014). Compared with the other two methods, direct pyrolysis of metal salt-loaded biomass (e.g. $FeCl_3$) has gained more attention because it is simple, effective, and favors the reactions that are reliable for the formation and attachment of magnetic particles to BC. During pyrolysis, surface functional groups and microstructure are also improved by the catalytic effect of $FeCl_3$, in parallel with adding the magnetization property to BC. In other words, activation and magnetization properties are simultaneously obtained during pyrolysis (Yang et al. 2016a,b). Reactions 80–85 explain the transformation of iron species during "direct pyrolysis." Magnetization starts with the hydrolysis of $FeCl_3$ loaded on biomass to $Fe(OH)_3$ and FeO(OH) through reactions 80 and 81. The generated FeO(OH) is then reduced to Fe_3O_4 through the three subsequent reactions of 82–84 at high temperature. Meanwhile, some reducing components such as CO, H_2, and amorphous carbon are formed. As the pyrolysis reaction proceeded under the high temperatures (~800°C), a portion of Fe_3O_4 may be transformed into Fe_3C due to the interaction with amorphous carbon. Reduction of residual $FeCl_3$ to $FeCl_2$ is also observed during the drying stage (through R85) (Yang et al. 2016a,b).

$$FeCl_3 + 3H_2O \rightarrow Fe(OH)_3 + 3HCl \quad (80)$$

$$Fe(OH)_3 \rightarrow FeO(OH) + H_2O \quad (81)$$

$$6FeO(OH) + H_2 \rightarrow 2Fe_3O_4 + 4H_2O \quad (82)$$

$$6FeO(OH) + 4CO \rightarrow 2Fe_3O_4 + 4CO_2 \quad (83)$$

$$6FeO(OH) + 4C \rightarrow 2Fe_3O_4 + 4CO \quad (84)$$

$$2FeCl_3 + H_2 \rightarrow 2FeCl_2 + 2HCl \quad (85)$$

As already mentioned, the magnetization of BC usually decreases the BET surface area due to the formation of secondary iron (hydro)oxides on the surface (Mohan et al. 2014, Wang et al. 2014). However, impregnation of biomass, prior to carbonization, may increase the surface area if a suitable biomass: iron ratio is selected. Mubarak et al. have reported that the BET surface area, pore volume, and yield of BC enhanced to a maximum (from 250 to 525 m^2/g) at an impregnation ratio of 0.5 ($FeCl_3$:biomass) and then decreased with further increases in the chemical ratio (Mubarak et al. 2016). It has also been reported that regeneration and reuse of magnetic BCs increase its S_{BET}, V_{mi}, V_{me}, V_t, and pH_{PZC} due to the dissolution of ash and the loss of iron oxides dispersed on the surface of MBC (Wang et al. 2015a,b).

5.7.1 Application

Enhancement of metal sorption on magnetically modified BCs has been extensively studied. Combination of ion exchange and metal chelation prevails the other mechanisms of metal sorption in magnetite BCs. Significant increment of metal chelation mechanism is attributed to the generation of new acidic functions (e.g. solid $Fe_xO_y(OH)$ anchored on the BC and the related groups) as well as the change of chemical properties (pH and PZC values) of all the pristine BCs after magnetic modification (Lu et al. 2012, Samsuri et al. 2014, Trakal et al. 2016). Negative sites created on both ferric oxide/Fe_3O_4 surfaces and char at high pH values enhance attractions and decrease repulsions between the sorbent surface and metal ions. In such condition, metal ions replace protons from the magnetic BC surfaces. In contrast, at low pH values, positive sites dominate the surface, increasing electrostatic repulsion between the sorbent surface and trace metal ions. It has been reported that cation exchange is also strengthened after Fe oxide impregnation, which limits the desorbed amount of trace metals (Lu et al. 2012, Samsuri et al. 2014, Trakal et al. 2016). Adsorption mechanisms at low and high pH values [202] are given below (where M^{2+} = heavy metal, e.g. Pb^{2+}, Cd^{2+}):

At low pH values:

For dehydrated ions:

$$Fe\text{-}OH + H_3O^+ \leftrightarrow Fe\text{-}OH_2^+ + H_2O \quad (86)$$

$$Fe\text{-}OH + M^{2+} \longleftrightarrow Fe\text{-}O^{M^{2+}}_{H} \longleftrightarrow Fe^-\text{-}O^{M^+}_{H} \quad (87)$$

For hydrated ions:

$$Fe\text{-}OH \overset{-OH}{\longleftrightarrow} Fe\text{-}O^- + H_2O \xrightarrow{M(OH_2)_n^{2+}} Fe\text{-}O\text{-}M(OH_2)_n \quad (88)$$

Oxygen bridge forms

At high pH values:

$$Fe\text{-}OH + H_2O \leftrightarrow Fe\text{-}O^- + H_3O^+ \quad (89)$$

$$H_3O^+ + OH^- \leftrightarrow 2H_2O \quad (90)$$

$$Fe\text{-}O^- + M[(OH-2)_{n-m}(OH)_m]^{(2-m)+} \leftrightarrow Fe\text{-}OM[(OH_2)_{n-m}(OH)_m]^{(2-m)+} \quad (91)$$

Generally, most BCs with relatively low pH_{PZC} (<4) and high alkalinity (pH 7–12) have a low anion exchange capacity (<5 cmol kg^{-1}), and hence, very limited sorption ability towards the negatively charged anions such as phosphate and As(V) (Cai et al. 2017). Magnetic modification of BC increases adsorption of such contaminants mainly by complexation via ligand exchange between surface -OH and anions (e.g. P anions, forming Fe-O-P bond) (Cai et al. 2017). As(V) and phosphate are chemical analogs with many similarities. Magnetic BC has also exhibited a notable capability to remove aqueous arsenate [As(V)] (98.46% removal), compared with pristine one (13.78% removal). Ligand exchange between As(V) anion and the hydroxylated surface of Fe_3O_4 as well as H bonds are largely responsible for As(V) sorption (Zhang et al. 2016a,b). Accordingly, reduction of As(V) removal with increasing pH (>10) is probably due to the higher competition between and $HAsO_4^{2-}$ and OH.

The magnetic BCs have also demonstrated a great potential for removal of various aromatic pollutants. As for metal adoptions, the adsorption mechanism depends mainly on magnetic BC properties and target contaminants. It has been reported that the magnetic BC with the grapheme like-structure has a higher p-electron density and hence these layers can be regarded as a π-electron donor which is the dominant mechanism for guaiacol adsorption on magnetic BCs, while pore-filling, surface area, and hydrophobic effect control the anisole adsorption (Li et al. 2017a,b,c,d). Magnetic BC-based polymers are among the newest composites synthesized. They exhibit a good potential (615 F/g) for future supercapacitor applications (Thines et al. 2016). The zero-valent iron magnetic BC composites have also been synthesized from

reducing Fe(II) to Fe(0) using $NaBH_4$ as a reducing agent and have demonstrated a great ability for the simultaneous adsorption and dechlorination of pentachlorophenol (Devi and Saroha 2014). Further manipulation of magnetic BC with sulfuric acid enhances the catalytic activity of the magnetic BC acid-catalyzed reactions such as esterification, dehydration, and hydrolysis (Liu et al. 2013b).

Table 1 summarizes all activation/modification methods investigated in this review article along with their effects on BC applications.

6 Conclusion

In the recent two decades, innovative methodologies have been applied to improve the physiochemical properties of biomass-derived chars. These efforts resulted in increasing their efficiency as adsorbents for wastewater treatment, supercapacitors, catalyst, etc. at a reasonable cost. Modifications of BCs are divided into two general groups. Physical modifications mainly affect physical structure while chemical modifications bear the major effect on BC chemical bonds and functional groups. This paper presents a comprehensive review on chemical modifications of BC for the first time. According to modification effect on BC functionalities, chemical modification can be further categorized into oxidation, amination, sulfonation, and impregnation of metal oxides into BC structure. This review explores in details the mechanisms of different chemical modifications, their effects on physiochemical properties of BC as well as on their application. The quantity of oxygen-containing functional groups on the carbonaceous surface increases by activation with oxidizing gases or using acidic or basic oxidizing solutions. In this paper, oxidation with phosphoric acid, nitric acid, activation with hydrochloric acid, hydrogen peroxide, sodium hydroxide, and potassium hydroxide is comprehensively elucidated. Surface sulfonation and amination which are among the most common methods to introduce sulfonic and amino groups into BC are also discussed in detail. In addition, impregnation of different metal (e.g. Mg, Mn, Ca, Cu, Ni, and Fe) oxides into BC structure which is considered as a cationic-modification and can enhance the efficiency, ability, and selectivity to anions adsorption are also revealed in our work. Among different metal oxides, induction of Fe containing ions donates the ferromagnetic property to BC. It provides effective adsorptivity, fast separation easy recycling, making this modification commercially vital. Magnetization with ferric and ferrous ions is reviewed in the last section of this work.

Acknowledgements: The authors are grateful for the financial support of the National Science Foundation (NSF EPSCoR RII grant no. OIA-1632899). Various other support from the University of Mississippi is also gratefully acknowledged.

References

Afkhami A, Madrakian T, Karimi Z. The effect of acid treatment of carbon cloth on the adsorption of nitrite and nitrate ions. J Hazard Mater 2007; 144: 427–431.

Agrafioti E, Kalderis D, Diamadopoulos E. Ca and Fe modified biochars as adsorbents of arsenic and chromium in aqueous solutions. J Environ Manage 2014; 146: 444–450.

Ahmed Hared I, Dirion J-L, Salvador S, Lacroix M, Rio S. Pyrolysis of wood impregnated with phosphoric acid for the production of activated carbon: kinetics and porosity development studies. J Anal Appl Pyrolysis 2007; 79: 101–105.

Ahmed MB, Zhou JL, Ngo HH, Guo W, Chen M. Progress in the preparation and application of modified biochar for improved contaminant removal from water and wastewater. Bioresour Technol 2016; 214: 836–851.

Al-Warhi TI, Al-Hazimi HMA, El-Faham A. Recent development in peptide coupling reagents. J Saudi Chem Soc 2012; 16: 97–116.

Almeida LC, Barbosa AS, Fricks AT, Freitas LS, Lima ÁS, Soares CMF. Use of conventional or non-conventional treatments of biochar for lipase immobilization. Process Biochem 2017; 61: 124–129

Álvarez PM, McLurgh D, Plucinski P. Copper oxide mounted on activated carbon as catalyst for wet air oxidation of aqueous phenol. 1. Kinetic and mechanistic approaches. Ind Eng Chem Res 2002a; 41: 2147–2152.

Álvarez PM, McLurgh D, Plucinski P. Copper oxide mounted on activated carbon as catalyst for wet air oxidation of aqueous phenol. 2. Catalyst stability. Ind Eng Chem Res 2002b; 41: 2153–2158.

Angın D, Altintig E, Köse TE. Influence of process parameters on the surface and chemical properties of activated carbon obtained from biochar by chemical activation. Bioresour Technol 2013; 148: 542–549.

Archanjo BS, Araujo JR, Silva AM, Capaz RB, Falcão NPS, Jorio A, Achete CA. Chemical analysis and molecular models for calcium–oxygen–carbon interactions in black carbon found in fertile amazonian anthrosoils. Environ Sci Technol 2014; 48: 7445–7452.

Argun ME, Dursun S, Ozdemir C, Karatas M. Heavy metal adsorption by modified oak sawdust: thermodynamics and kinetics. J Hazard Mater 2007; 141: 77–85.

Balakrishna S, Lomnicki S, McAvey KM, Cole RB, Dellinger B, Cormier SA. Environmentally persistent free radicals amplify ultrafine particle mediated cellular oxidative stress and cytotoxicity. Part Fibre Toxicol 2009; 6: 1743–8977.

Boehm HP. Chemical identification of surface groups. Adv Catal 1966; 16: 179–274.

Boehm HP. Surface oxides on carbon and their analysis: a critical assessment. Carbon 2002; 40: 145–149.

Broadley S, Vondrak T, Wright TG, Plane JMC. A kinetic study of Ca-containing ions reacting with O, O2, CO2 and H2O:

implications for calcium ion chemistry in the upper atmosphere. Phys Chem Chem Phys 2008; 10: 5287–5298.
Bundschuh J, Hollander HM, Ma LQ. In-situ remediation of arsenic-contaminated sites. London, UK: CRC Press, 2014: 15–16.
Byamba-Ochir N, Shim WG, Balathanigaimani MS, Moon H. Highly porous activated carbons prepared from carbon rich Mongolian anthracite by direct NaOH activation. Appl Surf Sci 2016; 379: 331–337.
Cai R, Wang X, Ji X, Peng B, Tan C, Huang X. Phosphate reclaim from simulated and real eutrophic water by magnetic biochar derived from water hyacinth. J Environ Manage 2017; 187: 212–219.
Cainelli G, Cardillo G. Oxidation of carbon-carbon double bonds, chromium oxidations in organic chemistry. Berlin, Heidelberg: Springer Berlin Heidelberg, 1984: 59–117.
Cameron A, MacDowall JD. The pore structure of wood based activated carbons, RILEMjCNR International Symposium, Milan, Italy, 1983:251.
Cazetta AL, Vargas AMM, Nogami EM, Kunita MH, Guilherme MR, Martins AC, Silva TL, Moraes JCG, Almeida VC. NaOH-activated carbon of high surface area produced from coconut shell: Kinetics and equilibrium studies from the methylene blue adsorption. Chem Eng J 2011; 174: 117–125.
Cazorla C, Shevlin SA, Guo ZX. Calcium-based functionalization of carbon materials for CO2 capture: a first-principles computational study. J Phys Chem C 2011; 115: 10990–10995.
Cha JS, Park SH, Jung S-C, Ryu C, Jeon J-K, Shin M-C, Park Y-K. Production and utilization of biochar: a review. J Ind Eng Chem 2016; 40: 1–15.
Changsuphan A, Wahab MIBA, Kim Oanh NT. Removal of benzene by ZnO nanoparticles coated on porous adsorbents in presence of ozone and UV. Chem Eng J 2012; 181: 215–221.
Chatterjee R, Sajjadi B, Mattern DL, Chen W-Y, Zubatiuk T, Leszczynska D, Leszczynski J, Egiebor NO, Hammer N. Ultrasound cavitation intensified amine functionalization: a feasible strategy for enhancing CO2 capture capacity of biochar. Fuel 2018; 225: 287–298.
Chen JP, Wu S. Acid/base-treated activated carbons: characterization of functional groups and metal adsorptive properties. Langmuir 2004; 20: 2233–2242.
Chiang H-L, Chiang PC, Huang CP. Ozonation of activated carbon and its effects on the adsorption of VOCs exemplified by methylethylketone and benzene. Chemosphere 2002; 47: 267–275.
Cho D-W, Kim S, Tsang YF, Song H. Preparation of nitrogen-doped Cu-biochar and its application into catalytic reduction of p-nitrophenol. Environ Geochem Health 2017.
Cibati A, Foereid B, Bissessur A, Hapca S. Assessment of Miscanthus × giganteus derived biochar as copper and zinc adsorbent: study of the effect of pyrolysis temperature, pH and hydrogen peroxide modification. J Clean Prod 2017; 162: 1285–1296.
Dai L, Tan F, Li H, Zhu N, He M, Zhu Q, Hu G, Wang L, Zhao J. Calcium-rich biochar from the pyrolysis of crab shell for phosphorus removal. J Environ Manage 2017; 198: 70–74.
Dalai AK, Azargohar R. Production of activated carbon from biochar using chemical and physical activation: mechanism and modeling, materials, chemicals, and energy from forest biomass. ACS 2007:463–476.
de Oliveira PR, Kalinke C, Gogola JL, Mangrich AS, Junior LHM, Bergamini MF. The use of activated biochar for development of a sensitive electrochemical sensor for determination of methyl parathion. J Electroanal Chem 2017; 799: 602–608.
Dellinger B, Lomnicki S, Khachatryan L, Maskos Z, Hall RW, Adounkpe J, McFerrin C, Truong H. Formation and stabilization of persistent free radicals. Proc Combust Inst 2007; 31: 521–528.
Demiral H, Demiral İ. Surface properties of activated carbon prepared from wastes. Surf Interface Anal 2008; 40: 612–615.
Devi P, Saroha AK. Synthesis of the magnetic biochar composites for use as an adsorbent for the removal of pentachlorophenol from the effluent. Bioresour Technol 2014; 169: 525–531.
Devi P, Saroha AK. Simultaneous adsorption and dechlorination of pentachlorophenol from effluent by Ni–ZVI magnetic biochar composites synthesized from paper mill sludge. Chem Eng J 2015; 271: 195–203.
Ding L, Zou B, Li Y, Liu H, Wang Z, Zhao C, Su Y, Guo Y. The production of hydrochar-based hierarchical porous carbons for use as electrochemical supercapacitor electrode materials. Colloids Surf A Physicochem Eng Asp 2013; 423: 104–111.
El-Hendawy A-NA. An insight into the KOH activation mechanism through the production of microporous activated carbon for the removal of Pb2 + cations. Appl Surf Sci 2009; 255: 3723–3730.
Elmouwahidi A, Bailón-García E, Pérez-Cadenas AF, Maldonado-Hódar FJ, Carrasco-Marín F. Activated carbons from KOH and H3PO4-activation of olive residues and its application as supercapacitor electrodes. Electrochim Acta 2017; 229: 219–228.
Fang C, Zhang T, Li P, Jiang RF, Wang YC. Application of magnesium modified corn biochar for phosphorus removal and recovery from swine wastewater. Int J Environ Res Public Health 2014a; 11: 9217–9237.
Fang G, Gao J, Liu C, Dionysiou DD, Wang Y, Zhou D. Key role of persistent free radicals in hydrogen peroxide activation by biochar: implications to organic contaminant degradation. Environ Sci Technol 2014b; 48: 1902–1910.
Fang C, Zhang T, Li P, Jiang R, Wu S, Nie H, Wang Y. Phosphorus recovery from biogas fermentation liquid by Ca–Mg loaded biochar. J Environ Sci 2015a; 29: 106–114.
Fang G, Liu C, Gao J, Dionysiou DD, Zhou D. Manipulation of persistent free radicals in biochar to activate persulfate for contaminant degradation. Environ Sci Technol 2015b; 49: 5645–5653.
Figueiredo JL, Pereira MFR, Freitas MMA, Órfão JJM. Modification of the surface chemistry of activated carbons. Carbon 1999; 37: 1379–1389.
Foo KY, Hameed BH. Coconut husk derived activated carbon via microwave induced activation: effects of activation agents, preparation parameters and adsorption performance. Chem Eng J 2012a; 184: 57–65.
Foo KY, Hameed BH. Potential of jackfruit peel as precursor for activated carbon prepared by microwave induced NaOH activation. Bioresour Technol 2012b; 112: 143–150.
Gan C, Liu Y, Tan X, Wang S, Zeng G, Zheng B, Li T, Jiang Z, Liu W. Effect of porous zinc-biochar nanocomposites on Cr(vi) adsorption from aqueous solution. RSC Adv 2015; 5: 35107–35115.
Georgi A, Kopinke F-D. Interaction of adsorption and catalytic reactions in water decontamination processes: part I. Oxidation of organic contaminants with hydrogen peroxide catalyzed by activated carbon. Appl Catal B: Environ 2005; 58: 9–18.

Ghaedi M, Karimi H, Yousefi F. Silver and zinc oxide nanostructures loaded on activated carbon as new adsorbents for removal of methylene green. Hum Exp Toxicol 2014; 33: 956–967.
Gholidoust A, Atkinson JD, Hashisho Z. Enhancing CO2 adsorption via amine-impregnated activated carbon from oil sands coke. Energy Fuels 2017; 31: 1756–1763.
Ghouma I, Jeguirim M, Sager U, Limousy L, Bennici S, Däuber E, Asbach C, Ligotski R, Schmidt F, Ouederni A. The potential of activated carbon made of agro-industrial residues in NOx immissions abatement. Energies 2017; 10: 1508.
Gokce Y, Aktas Z. Nitric acid modification of activated carbon produced from waste tea and adsorption of methylene blue and phenol. Appl Surf Sci 2014; 313: 352–359.
González ME, Cea M, Reyes D, Romero-Hermoso L, Hidalgo P, Meier S, Benito N, Navia R. Functionalization of biochar derived from lignocellulosic biomass using microwave technology for catalytic application in biodiesel production. Energy Convers Manag 2017; 137: 165–173.
Guo J, Lua AC. Textural characterization of activated carbons prepared from oil-palm stones pre-treated with various impregnating agents. J Porous Mat 1999; 7: 491–497.
Guo J, Xu WS, Chen YL, Lua AC. Adsorption of NH3 onto activated carbon prepared from palm shells impregnated with H2SO4. J Colloid Interface Sci 2005; 281: 285–290.
Güzel F, Sayğılı H, Akkaya Sayğılı G, Koyuncu F, Yılmaz C. Optimal oxidation with nitric acid of biochar derived from pyrolysis of weeds and its application in removal of hazardous dye methylene blue from aqueous solution. J Clean Prod 2017; 144: 260–265.
Hamid S, Chowdhury Z, Zain S. Base catalytic approach: a promising technique for the activation of biochar for equilibrium sorption studies of copper, Cu(II) ions in single solute system. Materials 2014; 7: 2815.
Han Y, Cao X, Ouyang X, Sohi SP, Chen J. Adsorption kinetics of magnetic biochar derived from peanut hull on removal of Cr (VI) from aqueous solution: effects of production conditions and particle size. Chemosphere 2016; 145: 336–341.
Harikishore Kumar Reddy D, Lee S-M. Magnetic biochar composite: facile synthesis, characterization, and application for heavy metal removal. Colloids Surf A Physicochem Eng Asp 2014; 454: 96–103.
Hasegawa G, Deguchi T, Kanamori K, Kobayashi Y, Kageyama H, Abe T, Nakanishi K. High-level doping of nitrogen, phosphorus, and sulfur into activated carbon monoliths and their electrochemical capacitances. Chem Mater 2015; 27: 4703–4712.
Heroux DS, Volodin AM, Zaikovski VI, Chesnokov VV, Bedilo AF, Klabunde KJ. ESR and HRTEM study of carbon-coated nanocrystalline MgO. J Phys Chem B 2004; 108: 3140–3144.
Hiemenz PC, Rajagopalan R. Principles of colloid and surface chemistry. Boca Raton: CRC Press, 1997.
Hilton R, Bick P, Tekeei A, Leimkuehler E, Pfeifer P, Suppes GJ. Mass balance and performance analysis of potassium hydroxide activated carbon. Ind Eng Chem Res 2012; 51: 9129–9135.
Huff MD, Lee JW. Biochar-surface oxygenation with hydrogen peroxide. J Environ Manage 2016; 165: 17–21.
Hulicova-Jurcakova D, Puziy AM, Poddubnaya OI, Suárez-García F, Tascón JMD, Lu GQ. Highly stable performance of supercapacitors from phosphorus-enriched carbons. J Am Chem Soc 2009; 131: 5026–5027.
Inoue Y, Yamasaki H, Nakamizo H. Studies of the hydrous tin(IV) oxide ion exchanger. The effect of heat treatment. Bull Chem Soc Jpn 1985; 58: 1292–1298.
Islam MA, Tan IAW, Benhouria A, Asif M, Hameed BH. Mesoporous and adsorptive properties of palm date seed activated carbon prepared via sequential hydrothermal carbonization and sodium hydroxide activation. Chem Eng J 2015; 270: 187–195.
Islam MA, Ahmed MJ, Khanday WA, Asif M, Hameed BH. Mesoporous activated carbon prepared from NaOH activation of rattan (Lacosperma secundiflorum) hydrochar for methylene blue removal. Ecotoxicol Environ Saf 2017; 138: 279–285.
Jagtoyen M, Derbyshire F. Some considerations of the origins of porosity in carbons from chemically activated wood. Carbon 1993; 31: 1185–1192.
Jagtoyen M, Derbyshire F. Activated carbons from yellow poplar and white oak by H3PO4 activation. Carbon 1998; 36: 1085–1097.
Jansen RJJ, van Bekkum H. Amination and ammoxidation of activated carbons. Carbon 1994; 32: 1507–1516.
Jaramillo J, Gómez-Serrano V, Álvarez PM. Enhanced adsorption of metal ions onto functionalized granular activated carbons prepared from cherry stones. J Hazard Mater 2009; 161: 670–676.
Jiang Z, Liu Y, Sun X, Tian F, Sun F, Liang C, You W, Han C, Li C. Activated carbons chemically modified by concentrated H2SO4 for the adsorption of the pollutants from wastewater and the dibenzothiophene from fuel oils. Langmuir 2003; 19: 731–736.
Jin H, Wang X, Gu Z, Polin J. Carbon materials from high ash biochar for supercapacitor and improvement of capacitance with HNO3 surface oxidation. J Power Sources 2013; 236: 285–292.
Jin H, Capareda S, Chang Z, Gao J, Xu Y, Zhang J. Biochar pyrolytically produced from municipal solid wastes for aqueous As(V) removal: adsorption property and its improvement with KOH activation. Bioresour Technol 2014; 169: 622–629.
Jin H, Hanif MU, Capareda S, Chang Z, Huang H, Ai Y. Copper(II) removal potential from aqueous solution by pyrolysis biochar derived from anaerobically digested algae-dairy-manure and effect of KOH activation. J Environ Chem Eng 2016; 4: 365–372.
Jin J, Li S, Peng X, Liu W, Zhang C, Yang Y, Han L, Du Z, Sun K, Wang X. HNO3 modified biochars for uranium (VI) removal from aqueous solution. Bioresour Technol 2018; 256: 247–253.
Johannes L, Joseph S. Biochar for environmental management: science, Technology and Implementation, 2015:976 (page 994).
Jung K-W, Ahn K-H. Fabrication of porosity-enhanced MgO/biochar for removal of phosphate from aqueous solution: application of a novel combined electrochemical modification method. Bioresour Technol 2016; 200: 1029–1032.
Jung K-W, Jeong T-U, Kang H-J, Chang J-S, Ahn K-H. Preparation of modified-biochar from Laminaria japonica: simultaneous optimization of aluminum electrode-based electro-modification and pyrolysis processes and its application for phosphate removal. Bioresour Technol 2016; 214: 548–557.
Kamegawa K, Nishikubo K, Yoshida H. Oxidative degradation of carbon blacks with nitric acid (I) – changes in pore and crystallographic structures. Carbon 1998; 36: 433–441.
Karagöz S, Tay T, Ucar S, Erdem M. Activated carbons from waste biomass by sulfuric acid activation and their use on methylene blue adsorption. Bioresour Technol 2008; 99: 6214–6222.
Khachatryan L, Vejerano E, Lomnicki S, Dellinger B. Environmentally persistent free radicals (EPFRs). 1. Generation of reactive

oxygen species in aqueous solutions. Environ Sci Technol 2011; 45: 8559–8566.
Khadiran T, Hussein MZ, Zainal Z, Rusli R. Textural and chemical properties of activated carbon prepared from tropical peat soil by chemical activation method, 2014.
Kikuchi Y, Qian Q, Machida M, Tatsumoto H. Effect of ZnO loading to activated carbon on Pb(II) adsorption from aqueous solution. Carbon 2006; 44: 195–202.
Kim B-S, Lee HW, Park SH, Baek K, Jeon J-K, Cho HJ, Jung S-C, Kim SC, Park Y-K. Removal of Cu2+ by biochars derived from green macroalgae. Environ Sci Pollut Res 2016; 23: 985–994.
Kleber M, Hockaday W, Nico PS. Characteristics of biochar: macro-molecular properties, Chapter 6. In: Lehmann J, Joseph S, editors. Biochar for environmental management: science and technology and implementation. New York: Routledge, 2015.
Koenig W, Geiger R. A new method for synthesis of peptides: activation of the carboxyl group with dicyclohexylcarbodiimide using 1-hydroxybenzotriazoles as additives. Chem Ber 1970; 103: 788.
Kostić MD, Bazargan A, Stamenković OS, Veljković VB, McKay G. Optimization and kinetics of sunflower oil methanolysis catalyzed by calcium oxide-based catalyst derived from palm kernel shell biochar. Fuel 2016; 163: 304–313.
Kuwata K, Saito Y, Shida S, Ohta M. Intercalation of wood charcoal with sulfuric acid. J Wood Sci 2009; 55: 154–158.
Lado JJ, Zornitta RL, Calvi FA, Martins M, Anderson MA, Nogueira FGE, Ruotolo LAM. Enhanced capacitive deionization desalination provided by chemical activation of sugar cane bagasse fly ash electrodes. J Anal Appl Pyrolysis 2017; 126: 143–153.
Lau AYT, Tsang DCW, Graham NJD, Ok YS, Yang X, Li X-d. Surface-modified biochar in a bioretention system for Escherichia coli removal from stormwater. Chemosphere 2017; 169: 89–98.
Leony Leon CA, Radovic L. Interfacial chemistry and electrochemistry of carbon surfaces. Chem Phys Carbon 1194; 24: 213–310.
Lewis GN, Bigeleisen J. Methylene blue and other indicators in general acids. The acidity function. J Am Chem Soc 1943; 65: 1144–1150.
Li F, Cao X, Zhao L, Wang J, Ding Z. Effects of mineral additives on biochar formation: carbon retention, stability, and properties. Environ Sci Technol 2014; 48: 11211–11217.
Li R, Wang JJ, Zhou B, Awasthi MK, Ali A, Zhang Z, Lahori AH, Mahar A. Recovery of phosphate from aqueous solution by magnesium oxide decorated magnetic biochar and its potential as phosphate-based fertilizer substitute. Bioresour Technol 2016a; 215: 209–214.
Li J, Zhang P, Wang J, Wang M. Birnessite-type manganese oxide on granular activated carbon for formaldehyde removal at room temperature. J Phys Chem C 2016b; 120: 24121–24129.
Li H, Mahyoub SAA, Liao W, Xia S, Zhao H, Guo M, Ma P. Effect of pyrolysis temperature on characteristics and aromatic contaminants adsorption behavior of magnetic biochar derived from pyrolysis oil distillation residue. Bioresour Technol 2017a; 223: 20–26.
Li H, Qiu Y-f, Wang X-l, Yang J, Yu Y-j, Chen Y-q, Liu Y-d. Biochar supported Ni/Fe bimetallic nanoparticles to remove 1,1,1-trichloroethane under various reaction conditions. Chemosphere 2017b; 169: 534–541.
Li R, Wang JJ, Zhou B, Zhang Z, Liu S, Lei S, Xiao R. Simultaneous capture removal of phosphate, ammonium and organic substances by MgO impregnated biochar and its potential use in swine wastewater treatment. J Clean Prod 2017c; 147: 96–107.
Li B, Yang L, Wang C-q, Zhang Q-p, Liu Q-c, Li Y-d, Xiao R. Adsorption of Cd(II) from aqueous solutions by rape straw biochar derived from different modification processes. Chemosphere 2017d; 175: 332–340.
Liang B, Lehmann J, Solomon D, Sohi S, Thies JE, Skjemstad JO, Luizão FJ, Engelhard MH, Neves EG, Wirick S. Stability of biomass-derived black carbon in soils. Geochim Cosmochim Acta 2008; 72: 6069–6078.
Liang J, Li X, Yu Z, Zeng G, Luo Y, Jiang L, Yang Z, Qian Y, Wu H. Amorphous MnO2 modified biochar derived from aerobically composted swine manure for adsorption of Pb(II) and Cd(II). ACS Sustain Chem Eng 2017; 5: 5049–5058.
Liao S, Pan B, Li H, Zhang D, Xing B. Detecting free radicals in biochars and determining their ability to inhibit the germination and growth of corn, wheat and rice seedlings. Environ Sci Technol 2014; 48: 8581–8587.
Lillo-Ródenas MA, Cazorla-Amorós D, Linares-Solano A. Understanding chemical reactions between carbons and NaOH and KOH: an insight into the chemical activation mechanism. Carbon 2003; 41: 267–275.
Lim WC, Srinivasakannan C, Balasubramanian N. Activation of palm shells by phosphoric acid impregnation for high yielding activated carbon. J Anal Appl Pyrolysis 2010; 88: 181–186.
Lin Y, Munroe P, Joseph S, Henderson R, Ziolkowski A. Water extractable organic carbon in untreated and chemical treated biochars. Chemosphere 2012; 87: 151–157.
Ling L-L, Liu W-J, Zhang S, Jiang H. Magnesium oxide embedded nitrogen self-doped biochar composites: fast and high-efficiency adsorption of heavy metals in an aqueous solution. Environ Sci Technol 2017; 51: 10081–10089.
Liu MY, Tsang DC, Hu J, Ng KT. Adsorption of methylene blue and phenol by wood waste derived activated carbon. J Environ Eng 2008; 134: 338–345.
Liu P, Liu W-J, Jiang H, Chen J-J, Li W-W, Yu H-Q. Modification of bio-char derived from fast pyrolysis of biomass and its application in removal of tetracycline from aqueous solution. Bioresour Technol 2012; 121: 235–240.
Liu W-J, Jiang H, Tian K, Ding Y-W, Yu H-Q. Mesoporous carbon stabilized mgo nanoparticles synthesized by pyrolysis of MgCl2 preloaded waste biomass for highly efficient CO2 capture. Environ Sci Technol 2013a; 47: 9397–9403.
Liu W-J, Tian K, Jiang H, Yu H-Q. Facile synthesis of highly efficient and recyclable magnetic solid acid from biomass waste. Sci Rep 2013b; 3: 2419–2426.
Liu S, Xu W-h, Liu Y-g, Tan X-f, Zeng G-m, Li X, Liang J, Zhou Z, Yan Z-l, Cai X-x. Facile synthesis of Cu(II) impregnated biochar with enhanced adsorption activity for the removal of doxycycline hydrochloride from water. Sci Total Environ 2017; 592: 546–553.
Lomnicki S, Truong H, Vejerano E, Dellinger B. Copper oxide-based model of persistent free radical formation on combustion-derived particulate matter. Environ Sci Technol 2008; 42: 4982–4988.
Low KS, Lee CK, Liew SC. Sorption of cadmium and lead from aqueous solutions by spent grain. Process Biochem 2000; 36: 59–64.
Lozano-Castelló D, Calo JM, Cazorla-Amorós D, Linares-Solano A. Carbon activation with KOH as explored by temperature

programmed techniques, and the effects of hydrogen. Carbon 2007; 45: 2529–2536.
Lu H, Reddy EP, Smirniotis PG. Calcium oxide based sorbents for capture of carbon dioxide at high temperatures. Ind Eng Chem Res 2006; 45: 3944–3949.
Lu H, Zhang W, Yang Y, Huang X, Wang S, Qiu R. Relative distribution of Pb2+ sorption mechanisms by sludge-derived biochar. Water Res 2012; 46: 854–862.
Machida M, Yamazaki R, Aikawa M, Tatsumoto H. Role of minerals in carbonaceous adsorbents for removal of Pb(II) ions from aqueous solution. Sep Purif Technol 2005; 46: 88–94.
Machida M, Mochimaru T, Tatsumoto H. Lead(II) adsorption onto the graphene layer of carbonaceous materials in aqueous solution. Carbon 2006; 44: 2681–2688.
Madzaki H, KarimGhani, WAWAB, NurZalikhaRebitanim, AzilBahariAlias. Carbon dioxide adsorption on sawdust biochar. Procedia Eng 2016; 148: 718–725.
Mahmoud DK, Salleh MAM, Karim WAWA, Idris A, Abidin ZZ. Batch adsorption of basic dye using acid treated kenaf fibre char: Equilibrium, kinetic and thermodynamic studies. Chem Eng J 2012; 181: 449–457.
Mao H, Zhou D, Hashisho Z, Wang S, Chen H, Wang H. Preparation of pinewood- and wheat straw-based activated carbon via a microwave-assisted potassium hydroxide treatment and an analysis of the effects of the microwave activation conditions, 2014.
Marrakchi F, Ahmed MJ, Khanday WA, Asif M, Hameed BH. Mesoporous-activated carbon prepared from chitosan flakes via single-step sodium hydroxide activation for the adsorption of methylene blue. Int J Biol Macromol 2017; 98: 233–239.
Mascolo MC, Pei Y, Ring TA. Room temperature co-precipitation synthesis of magnetite nanoparticles in a large pH window with different bases. Materials 2013; 6: 5549–5567.
Mitani S, Lee S-I, Yoon S-H, Korai Y, Mochida I. Activation of raw pitch coke with alkali hydroxide to prepare high performance carbon for electric double layer capacitor. J Power Sources 2004; 133: 298–301.
Miyawaki J, Lee G-H, Yeh J, Shiratori N, Shimohara T, Mochida I, Yoon S-H. Development of carbon-supported hybrid catalyst for clean removal of formaldehyde indoors. Catal Today 2012; 185: 278–283.
Mohan D, Kumar H, Sarswat A, Alexandre-Franco M, Pittman CU. Cadmium and lead remediation using magnetic oak wood and oak bark fast pyrolysis bio-chars. Chem Eng J 2014; 236: 513–528.
Mohan D, Singh P, Sarswat A, Steele PH, Pittman CU. Lead sorptive removal using magnetic and nonmagnetic fast pyrolysis energy cane biochars. J Colloid Interface Sci 2015; 448: 238–250.
Montalbetti CA, Falque V. Amide bond formation and peptide coupling. Tetrahedron 2005; 61: 10827–10852.
Montes-Morán MA, Menéndez JA, Fuente E, Suárez D. Contribution of the basal planes to carbon basicity: an ab initio study of the H3O+–π interaction in cluster models. J Phys Chem B 1998; 102: 5595–5601.
Montes-Morán MA, Suárez D, Menéndez JA, Fuente E. On the nature of basic sites on carbon surfaces: an overview. Carbon 2004; 42: 1219–1225.
Mubarak NM, Sahu JN, Abdullah EC, Jayakumar NS. Plam oil empty fruit bunch based magnetic biochar composite comparison for synthesis by microwave-assisted and conventional heating. J Anal Appl Pyrolysis 2016; 120: 521–528.
Nair V, Vinu R. Peroxide-assisted microwave activation of pyrolysis char for adsorption of dyes from wastewater. Bioresour Technol 2016; 216: 511–519.
Nasernejad B, Zadeh TE, Pour BB, Bygi ME, Zamani A. Camparison for biosorption modeling of heavy metals (Cr (III), Cu (II), Zn (II)) adsorption from wastewater by carrot residues. Process Biochem 2005; 40: 1319–1322.
Ngarmkam W, Sirisathitkul C, Phalakornkule C. Magnetic composite prepared from palm shell-based carbon and application for recovery of residual oil from POME. J Environ Manage 2011; 92: 472–479.
Nguyen TTN, Xu C-Y, Tahmasbian I, Che R, Xu Z, Zhou X, Wallace HM, Bai SH. Effects of biochar on soil available inorganic nitrogen: a review and meta-analysis. Geoderma 2017; 288: 79–96.
Niu R, Li H, Ma Y, He L, Li J. An insight into the improved capacitive deionization performance of activated carbon treated by sulfuric acid. Electrochim Acta 2015; 176: 755–762.
Noraini MN, Abdullah EC, Othman R, Mubarak NM. Single-route synthesis of magnetic biochar from sugarcane bagasse by microwave-assisted pyrolysis. Mater Lett 2016; 184: 315–319.
Nourmoradi H, Ghiasvand AR, Noorimotlagh Z. Removal of methylene blue and acid orange 7 from aqueous solutions by activated carbon coated with zinc oxide (ZnO) nanoparticles: equilibrium, kinetic, and thermodynamic study. Desalin Water Treat 2015; 55: 252–262.
Ok YS, Uchimiya SM, Chang SX, Bolan N. Biochar: production, characterization, and applications. Boca Raton, FL: CRC Press, Taylor and Francis Group, 2015.
Orlando US, Baes AU, Nishijima W, Okada M. Preparation of agricultural residue anion exchangers and its nitrate maximum adsorption capacity. Chemosphere 2002; 48: 1041–1046.
Otowa T, Nojima Y, Miyazaki T. Development of KOH activated high surface area carbon and its application to drinking water purification. Carbon 1997; 35: 1315–1319.
Pandey SN, Nair P. Effect of phosphoric acid treatment on physical and chemical properties of cotton fiber1. Text Res J 1974; 44: 927–933.
Park SJ, Jang YS. Pore structure and surface properties of chemically modified activated carbons for adsorption mechanism and rate of Cr(VI). J Colloid Interface Sci 2002; 249: 458–463.
Park G-G, Yang T-H, Yoon Y-G, Lee W-Y, Kim C-S. Pore size effect of the DMFC catalyst supported on porous materials. Int J Hydrogen Energy 2003; 28: 645–650.
Patnukao P, Pavasant P. Activated carbon from Eucalyptus camaldulensis Dehn bark using phosphoric acid activation. Bioresour Technol 2008; 99: 8540–8543.
Peng H, Gao P, Chu G, Pan B, Peng J, Xing B. Enhanced adsorption of Cu(II) and Cd(II) by phosphoric acid-modified biochars. Environ Pollut 2017; 229: 846–853.
Perrin A, Celzard A, Albiniak A, Kaczmarczyk J, Marêché JF, Furdin G. NaOH activation of anthracites: effect of temperature on pore textures and methane storage ability. Carbon 2004; 42: 2855–2866.
Plane JMC, Rollason RJ. Kinetic study of the reactions of CaO with H2O, CO2, O2, and O3: implications for calcium chemistry in the mesosphere. J Phys Chem A 2001; 105: 7047–7056.
Porter BR, Rollins ML. Changes in porosity of treated lint cotton fibers. I. Purification and swelling treatments. J Appl Polym Sci 1972; 16: 217–236.
Przepiórski J, Czyżewski A, Pietrzak R, Morawski AW. MgO/CaO-loaded activated carbon for carbon dioxide capture:

practical aspects of use. Ind Eng Chem Res 2013; 52: 6669–6677.
Pu Y, Hu F, Huang F, Davison BH, Ragauskas AJ. Assessing the molecular structure basis for biomass recalcitrance during dilute acid and hydrothermal pretreatments. Biotechnol Biofuels 2013; 6: 1754–6834.
Purnomo CW, Salim C, Hinode H. Preparation and characterization of activated carbon from bagasse fly ash. J Anal Appl Pyrolysis 2011; 91: 257–262.
Purnomo CW, Salim C, Hinode H. Effect of the activation method on the properties and adsorption behavior of bagasse fly ash-based activated carbon. Fuel Process Technol 2012; 102: 132–139.
Radovic LR. Carbon materials in catalysis. Chem Phys Carbon 1997; 25: 243–358.
Radovic LR, Moreno-Castilla C, Rivera-Utrilla J. Carbon materials as adsorbents in aqueous solutions. Chem Phys Carbon 2001; 27: 227–406.
Ramsurn H, Kumar S, Gupta RB. Enhancement of biochar gasification in alkali hydrothermal medium by passivation of inorganic components using Ca(OH)2. Energy Fuels 2011; 25: 2389–2398.
Reddy DRK, Anitha S, Umadevi S. Kantowski-Sachs bulk viscous string cosmological model in f(R,T) gravity. Eur Phys J Plus 2014; 129: 96.
Reguyal F, Sarmah AK, Gao W. Synthesis of magnetic biochar from pine sawdust via oxidative hydrolysis of FeCl2 for the removal sulfamethoxazole from aqueous solution. J Hazard Mater 2017; 321: 868–878.
Roldán S, Villar I, Ruíz V, Blanco C, Granda M, Menéndez R, Santamaría R. Comparison between electrochemical capacitors based on NaOH- and KOH-activated carbons. Energy Fuels 2010; 24: 3422–3428.
Rostamian R, Heidarpour M, Mousavi SF, Afyuni M. Characterization and sodium sorption capacity of biochar and activated carbon prepared from rice husk. J Agr Sci Technol 2015; 17: 1057–1069.
Rufford TE, Hulicova-Jurcakova D, Zhu Z, Lu GQ. Nanoporous carbon electrode from waste coffee beans for high performance supercapacitors. Electrochem Commun 2008; 10: 1594–1597.
Rufford TE, Hulicova-Jurcakova D, Khosla K, Zhu Z, Lu GQ. Microstructure and electrochemical double-layer capacitance of carbon electrodes prepared by zinc chloride activation of sugar cane bagasse. J Power Sources 2010; 195: 912–918.
Samsuri AW, Sadegh-Zadeh F, Seh-Bardan BJ. Characterization of biochars produced from oil palm and rice husks and their adsorption capacities for heavy metals. Int J Environ Sci Technol 2014; 11: 967–976.
Sánchez-Polo M, Rivera-Utrilla J. Adsorbent – adsorbate interactions in the adsorption of Cd(II) and Hg(II) on ozonized activated carbons. Environ Sci Technol 2002; 36: 3850–3854.
Santos VP, Pereira MFR, Faria PCC, Órfão JJM. Decolourisation of dye solutions by oxidation with H2O2 in the presence of modified activated carbons. J Hazard Mater 2009; 162: 736–742.
Santos EM, Teixeira APdC, da Silva FG, Cibaka TE, Araújo MH, Oliveira WXC, Medeiros F, Brasil AN, de Oliveira LS, Lago RM. New heterogeneous catalyst for the esterification of fatty acid produced by surface aromatization/sulfonation of oilseed cake. Fuel 2015; 150: 408–414.
Sajjadi B, Chen WY, Egiebor NO. A comprehensive of biochar for energy and environmental applications. Rev Chem Eng 2018 (in press). DOI: https://doi.org/10.1515/revce-2017-0113.
Shafeeyan MS, Daud WMAW, Houshmand A, Shamiri A. A review on surface modification of activated carbon for carbon dioxide adsorption. J Anal Appl Pyrolysis 2010; 89: 143–151.
Shahkarami S, Dalai AK, Soltan J. Enhanced CO2 adsorption using MgO-impregnated activated carbon: impact of preparation techniques. Ind Eng Chem Res 2016; 55: 5955–5964.
Shan D, Deng S, Zhao T, Wang B, Wang Y, Huang J, Yu G, Winglee J, Wiesner MR. Preparation of ultrafine magnetic biochar and activated carbon for pharmaceutical adsorption and subsequent degradation by ball milling. J Hazard Mater 2016; 305: 156–163.
Shen Y, Areeprasert C, Prabowo B, Takahashi F, Yoshikawa K. Metal nickel nanoparticles in situ generated in rice husk char for catalytic reformation of tar and syngas from biomass pyrolytic gasification. RSC Adv 2014; 4: 40651–40664.
Shi K-y, Tao X-x, Hong F-f, He H, Ji Y-h, Li J-l. Mechanism of oxidation of low rank coal by nitric acid. J Coal Sci Eng (China) 2012; 18: 396–399.
Squadrito GL, Cueto R, Dellinger B, Pryor WA. Quinoid redox cycling as a mechanism for sustained free radical generation by inhaled airborne particulate matter. Free Radic Biol Med 2001; 31: 1132–1138.
Subramanian V, Luo C, Stephan AM, Nahm KS, Thomas S, Wei B. Supercapacitors from activated carbon derived from banana fibers. J Phys Chem C 2007; 111: 7527–7531.
Sumaraj, Padhye LP. Influence of surface chemistry of carbon materials on their interactions with inorganic nitrogen contaminants in soil and water. Chemosphere 2017; 184: 532–547.
Sun X, Cheng P, Wang H, Xu H, Dang L, Liu Z, Lei Z. Activation of graphene aerogel with phosphoric acid for enhanced electrocapacitive performance. Carbon 2015; 92: 1–10.
Taha SM, Amer ME, Elmarsafy AE, Elkady MY. Adsorption of 15 different pesticides on untreated and phosphoric acid treated biochar and charcoal from water. J Environ Chem Eng 2014; 2: 2013–2025.
Thines KR, Abdullah EC, Ruthiraan M, Mubarak NM, Tripathi M. A new route of magnetic biochar based polyaniline composites for supercapacitor electrode materials. J Anal Appl Pyrolysis 2016; 121: 240–257.
Tong Y, Mayer BK, McNamara PJ. Triclosan adsorption using wastewater biosolids-derived biochar. Environ Sci: Water Res Technol 2016; 2: 761–768.
Trakal L, Veselská V, Šafařík I, Vítková M, Číhalová S, Komárek M. Lead and cadmium sorption mechanisms on magnetically modified biochars. Bioresour Technol 2016; 203: 318–324.
Tsang DCW, Hu J, Liu MY, Zhang W, Lai KCK, Lo IMC. Activated carbon produced from waste wood pallets: adsorption of three classes of dyes. Water Air Soil Pollut 2007; 184: 141–155.
Tseng R-L. Mesopore control of high surface area NaOH-activated carbon. J Colloid Interface Sci 2006; 303: 494–502.
Tseng R-L, Tseng S-K. Pore structure and adsorption performance of the KOH-activated carbons prepared from corncob. J Colloid Interface Sci 2005; 287: 428–437.
Uchimiya M, Bannon DI, Wartelle LH. Retention of heavy metals by carboxyl functional groups of biochars in small arms range soil. J Agric Food Chem 2012; 60: 1798–1809.
Unnikrishnan B, Wu C-W, Chen IWP, Chang H-T, Lin C-H, Huang C-C. Carbon dot-mediated synthesis of manganese oxide decorated graphene nanosheets for supercapacitor application. ACS Sustainable Chem Eng 2016; 4: 3008–3016.

Wan C, Jiao Y, Li J. Core-shell composite of wood-derived biochar supported MnO2 nanosheets for supercapacitor applications. RSC Adv 2016; 6: 64811–64817.

Wang N, Wu C, Li J, Dong G, Guan L. Binder-free manganese oxide/carbon nanomaterials thin film electrode for supercapacitors. ACS Appl Mater Interfaces 2011; 3: 4185–4189.

Wang S-y, Tang Y-k, Li K, Mo Y-y, Li H-f, Gu Z-q. Combined performance of biochar sorption and magnetic separation processes for treatment of chromium-contained electroplating wastewater. Bioresour Technol 2014; 174: 67–73.

Wang S, Gao B, Li Y, Mosa A, Zimmerman AR, Ma LQ, Harris WG, Migliaccio KW. Manganese oxide-modified biochars: preparation, characterization, and sorption of arsenate and lead. Bioresour Technol 2015a; 181: 13–17.

Wang S-y, Tang Y-k, Chen C, Wu J-t, Huang Z, Mo Y-y, Zhang K-x, Chen J-b. Regeneration of magnetic biochar derived from eucalyptus leaf residue for lead(II) removal. Bioresour Technol 2015b; 186: 360–364.

Wang S, Gao B, Li Y. Enhanced arsenic removal by biochar modified with nickel (Ni) and manganese (Mn) oxyhydroxides. J Ind Eng Chem 2016a; 37: 361–365.

Wang Y-Y, Lu H-H, Liu Y-X, Yang S-M. Ammonium citrate-modified biochar: an adsorbent for La(III) ions from aqueous solution. Colloids Surf A Physicochem Eng Asp 2016b; 509: 550–563.

Wang P, Tang L, Wei X, Zeng G, Zhou Y, Deng Y, Wang J, Xie Z, Fang W. Synthesis and application of iron and zinc doped biochar for removal of p-nitrophenol in wastewater and assessment of the influence of co-existed Pb(II). Appl Surf Sci 2017a; 392: 391–401.

Wang Y, Zhang Y, Pei L, Ying D, Xu X, Zhao L, Jia J, Cao X. Converting Ni-loaded biochars into supercapacitors: implication on the reuse of exhausted carbonaceous sorbents. Sci Rep 2017b; 7: 41523–41531.

Wu F-C, Tseng R-L, Juang R-S. Comparisons of porous and adsorption properties of carbons activated by steam and KOH. J Colloid Interface Sci 2005; 283: 49–56.

Xia D, Tan F, Zhang C, Jiang X, Chen Z, Li H, Zheng Y, Li Q, Wang Y. ZnCl2-activated biochar from biogas residue facilitates aqueous As(III) removal. Appl Surf Sci 2016; 377: 361–369.

Xu X, Zhao Y, Sima J, Zhao L, Mašek O, Cao X. Indispensable role of biochar-inherent mineral constituents in its environmental applications: a review. Bioresour Technol 2017; 241: 887–899.

Xue Y, Gao B, Yao Y, Inyang M, Zhang M, Zimmerman AR, Ro KS. Hydrogen peroxide modification enhances the ability of biochar (hydrochar) produced from hydrothermal carbonization of peanut hull to remove aqueous heavy metals: batch and column tests. Chem Eng J 2012; 200–202: 673–680.

Yakout SM. Monitoring the changes of chemical properties of rice straw–derived biochars modified by different oxidizing agents and their adsorptive performance for organics. Bioremediat J 2015; 19: 171–182.

Yakout SM, Daifullah AEHM, El-Reefy SA. Pore structure characterization of chemically modified biochar derived from rice straw. Environ Eng Manag J 2015; 14: 8.

Yang G-X, Jiang H. Amino modification of biochar for enhanced adsorption of copper ions from synthetic wastewater. Water Res 2014; 48: 396–405.

Yang H, Yan R, Chen H, Zheng C, Lee DH, Liang DT. In-depth investigation of biomass pyrolysis based on three major components: hemicellulose, cellulose and lignin. Energy Fuels 2006; 20: 388–393.

Yang K, Peng J, Srinivasakannan C, Zhang L, Xia H, Duan X. Preparation of high surface area activated carbon from coconut shells using microwave heating. Bioresour Technol 2010; 101: 6163–6169.

Yang R, Liu G, Xu X, Li M, Zhang J, Hao X. Surface texture, chemistry and adsorption properties of acid blue 9 of hemp (Cannabis sativa L.) bast-based activated carbon fibers prepared by phosphoric acid activation. Biomass Bioenergy 2011; 35: 437–445.

Yang J, Pan B, Li H, Liao S, Zhang D, Wu M, Xing B. Degradation of p-nitrophenol on biochars: role of persistent free radicals. Environ Sci Technol 2016a; 50: 694–700.

Yang J, Zhao Y, Ma S, Zhu B, Zhang J, Zheng C. Mercury removal by magnetic biochar derived from simultaneous activation and magnetization of sawdust. Environ Sci Technol 2016b; 50: 12040–12047.

Yang J, Pignatello JJ, Pan B, Xing B. Degradation of p-nitrophenol by lignin and cellulose chars: H2O2-mediated reaction and direct reaction with the char. Environ Sci Technol 2017; 51: 8972–8980.

Yi J, Qing Y, Wu C, Zeng Y, Wu Y, Lu X, Tong Y. Lignocellulose-derived porous phosphorus-doped carbon as advanced electrode for supercapacitors. J Power Sources 2017; 351: 130–137.

Yu JT, Dehkhoda AM, Ellis N. Development of biochar-based catalyst for transesterification of canola oil. Energy Fuels 2011; 25: 337–344.

Yu Z, Zhou L, Huang Y, Song Z, Qiu W. Effects of a manganese oxide-modified biochar composite on adsorption of arsenic in red soil. J Environ Manage 2015; 163: 155–162.

Zawadzki J. IR spectroscopic investigations of the mechanism of oxidation of carbonaceous films with HNO3 solution. Carbon 1980; 18: 281–285.

Zhang M, Gao B. Removal of arsenic, methylene blue, and phosphate by biochar/AlOOH nanocomposite. Chem Eng J 2013; 226: 286–292.

Zhang ZG, Kyotani T, Tomita A. Dynamic behavior of surface oxygen complexes during oxygen-chemisorption and subsequent temperature-programmed desorption of calcium-loaded coal chars. Energy Fuels 1989; 3: 566–571.

Zhang QL, Lin YC, Chen X, Gao NY. A method for preparing ferric activated carbon composites adsorbents to remove arsenic from drinking water. J Hazard Mater 2007; 148: 671–678.

Zhang M, Gao B, Yao Y, Xue Y, Inyang M. Synthesis of porous MgO-biochar nanocomposites for removal of phosphate and nitrate from aqueous solutions. Chem Eng J 2012; 210: 26–32.

Zhang M, Gao B, Yao Y, Inyang M. Phosphate removal ability of biochar/MgAl-LDH ultra-fine composites prepared by liquid-phase deposition. Chemosphere 2013; 92: 1042–1047.

Zhang Z, Li J, Sun J, Wang H, Wei W, Sun Y. Bimodal mesoporous carbon-coated MgO nanoparticles for CO2 capture at moderate temperature conditions. Ind Eng Chem Res 2016a; 55: 7880–7887.

Zhang F, Wang X, Xionghui J, Ma L. Efficient arsenate removal by magnetite-modified water hyacinth biochar. Environ Pollut 2016b; 216: 575–583.

Zhao X, Zhang L, Murali S, Stoller MD, Zhang Q, Zhu Y, Ruoff RS. Incorporation of manganese dioxide within ultraporous

activated graphene for high-performance electrochemical capacitors. ACS Nano 2012; 6: 5404–5412.
Zhao L, Cao X, Zheng W, Scott JW, Sharma BK, Chen X. Copyrolysis of biomass with phosphate fertilizers to improve biochar carbon retention, slow nutrient release, and stabilize heavy metals in soil. ACS Sustainable Chem Eng 2016; 4: 1630–1636.
Zhou L, He J, Zhang J, He Z, Hu Y, Zhang C, He H. Facile in-situ synthesis of manganese dioxide nanosheets on cellulose fibers and their application in oxidative decomposition of formaldehyde. J Phys Chem C 2011; 115: 16873–16878.
Zhu D, Pignatello JJ. Characterization of aromatic compound sorptive interactions with black carbon (charcoal) assisted by graphite as a model. Environ Sci Technol 2005; 39: 2033–2041.
Zhu X, Liu Y, Qian F, Zhou C, Zhang S, Chen J. Preparation of magnetic porous carbon from waste hydrochar by simultaneous activation and magnetization for tetracycline removal. Bioresour Technol 2014; 154: 209–214.
Zuo X, Liu Z, Chen M. Effect of H2O2 concentrations on copper removal using the modified hydrothermal biochar. Bioresour Technol 2016; 207: 262–267.

Bionotes

Baharak Sajjadi
Department of Chemical Engineering, University of Mississippi, University, MS 38677, USA,
bsajjadi@olemiss.edu

Baharak Sajjadi is a research assistant professor at the University of Mississippi. She received her Master's degree in Chemical Engineering and completed her PhD in Bioprocess Engineering in 2015. Her main areas of research include computational fluid dynamic (CFD) simulation, energy and environment, bioenergy and biofuels and sono-physics. She has published more than 40 papers in high impact research journals since she received her BS degree in 2008.

Tetiana Zubatiuk
Interdisciplinary Center for Nanotoxicity, Jackson State University, 1400 J. R. Lynch Street, Jackson, MS 39217, USA

Tetiana Zubatiuk is a post-doc research associate in the Department of Chemistry, Physics, and Atmospheric Science at the Jackson State University. She has an experience in computational chemistry for 8 years. She researches a range of topics in electronic structure studies, dealing with properties and structure of DNA fragments and computational chemistry methods in environmental problems, surface chemistry, and atmospheric chemistry. She has published 13 research articles and 2 book chapters to date.

Danuta Leszczynska
Interdisciplinary Center for Nanotoxicity, Jackson State University, 1400 J. R. Lynch Street, Jackson, MS 39217, USA

Danuta Leszczynska is a professor of Environmental Engineering in the Department of Civil and Environmental Engineering at the Jackson State University. Her current research concentrates on the engineered or modified natural nano-sized materials in environment. She has served as a PI or co-PI of projects over 1 M. Her achievements include authoring over 200 peer reviewed publications, being Fulbright Scholar, member of National Academy of Inventors, and Distinguish Alumni.

Jerzy Leszczynski
Interdisciplinary Center for Nanotoxicity, Jackson State University, 1400 J. R. Lynch Street, Jackson, MS 39217, USA

Jerzy Leszczynski Professor of Chemistry and President's Distinguished Fellow at the Jackson State University, directs the Interdisciplinary Nanotoxicity NSF CREST Center. Dr. Leszczynski is a computational quantum chemist. He applies computational chemistry methods to a variety of research areas. He has published over 900 referred papers and 70 book chapters. Dr. Leszczynski is editor of several book series: *Computational chemistry: reviews of current trends*; *Challenges and advances in computational chemistry and physics*; *Practical aspects of computational chemistry*; editor of *Handbook of computational chemistry*; and series editor for *Lecture notes in chemistry*.

Wei Yin Chen
Department of Chemical Engineering, University of Mississippi, University, MS 38677, USA

Wei Yin Chen is a professor of Chemical Engineering at the University of Mississippi (UM). He has over 4 decades experience in carbon conversion and pollution control, and has served as a PI or co-PI of projects over $10 M. He established the Sustainable Energy & Environment Group (SEEG) at UM. SEEG is now part of the $6 M consortium for the sustainability in water/energy/food (WEF) nexus. His recent interests focus on low-energy modification of carbon for WEF applications.